이학박사 학위논문

Molecular mechanisms for thermostable circadian clock in *Arabidopsis* and thigmomorphogenetic responses to environmental changes in *Brachypodium*

애기장대 생체시계 고온 안정성과 환경 변화에 대한 숲개밀의 접촉형태형성 반응 기작 연구

2019년 8월

서울대학교 대학원

화학부

길 경 은

Molecular mechanisms for thermostable circadian clock in *Arabidopsis* and thigmomorphogenetic responses to environmental changes in *Brachypodium*

지도 교수 박 충 모

이 논문을 이학박사 학위논문으로 제출함
2019년 6월

서울대학교 대학원
화학부
길 경 은

길경은의 이학박사 학위논문을 인준함
2019년 6월

위 원 장 趙 章 澤 (인)

부위원장 박 충 모 (인)

위 원 이 형 호 (인)

위 원 윤 대 진 (인)

위 원 김 옥 매 (인)

ABSTRACT

It is widely perceived that plants are influenced by surrounding environment. The representative environmental stimuli are light, temperature fluctuation, and mechanical touch, such as rubbing and bending by passing animals, wind, and flooding. Plants have developed various adaptation strategies to cope with the environmental changes. For example, the circadian clock predicts the environmental changes and generates diurnal rhythms of numerous physiological and developmental processes in most living organisms to synchronize with surrounding conditions. In this study, I investigated the molecular mechanisms that contribute to thermostability of circadian clock in *Arabidopsis*.

Otherwise, some environmental stimuli, such as touch or wind, induce the morphological changes as well as clock rhythm of plants. The adaptive growth which accompanies with morphological changes is termed thigmomorphogenesis. Thigmomorphogenesis has been reported in the early stage of plant research, but the noticeable studies are not shown recently. Here, I described the phenotypic analysis of *Brachypodium* root formation under windy conditions. And hormonal regulation underlying the root development mechanisms in monocotyledon plants was also proposed.

In chapter 1, a role of ZEITLUPE (ZTL) in protein quality control under

heat stress is described. Cellular proteins undergo denaturation and oxidative damages under heat stress, forming insoluble aggregates that are toxic to cells. Denatured proteins are either renatured to their native conformations or removed from cellular compartments, which are processes often termed as protein quality control. Heat shock proteins (HSPs) act as molecular chaperones that assist the renaturation-degradation process. Here, I demonstrated that heat-induced protein aggregates are removed by a protein quality control system that includes the ZTL, a central clock component in *Arabidopsis*. ZTL mediates the polyubiquitination of aggregated proteins, which leads to proteasomal degradation, and enhances the thermotolerance of plants growing at high temperatures. Insufficient heat-induced polyubiquitination in *ztl-105* results in increased protein aggregates thus, thermosensitive phenotype. Notably, the circadian clock was hypersensitive to heat in the *ztl-105* mutant. I propose that ZTL-mediated protein quality control contributes to thermal stability of the clock. Moreover, the reduced levels of polyubiquitination and thermosensitive circadian clock in HSP90 RNAi plants indicate that HSP90 and ZTL are functionally related at high temperatures.

In chapter 2, influence of wind stimulation and adventitious root formation are discussed. Wind-driven mechanical stimulation is known to induce the incidence of radial expansion and shorter and stockier statue. Wind stimulation also affects the adaptive propagation of the root system in various plant species.

However, it is unknown how plants sense and transmit the wind-derived mechanical signals to launch appropriate responses, leading to the wind-adaptive root growth. Here, I found that *Brachypodium distachyon*, a model grass widely used for studies on bioenergy crops and cereals, efficiently adapts to wind-driven mechanical stress by forming adventitious roots (ARs), which are formed from nonroot tissues. The ARs prevent the leaf flipping of the plants by anchoring in soil. Experimental dissection of wind stimuli revealed that not the bending of the mesocotyls but physical contact of leaf nodes with soil triggers AR formation. Moreover, it was observed that inhibition of auxin transport is critical for AR emergence and/or elongation. Wind stimulation triggers the transcriptional induction of a group of auxin-responsive genes encoding WUSCHEL RELATED HOMEOBOX and LATERAL ORGAN BOUNDARIES DOMAIN transcription factors, which are intimately associated with the induction of AR formation. My findings would contribute to further understanding molecular mechanisms governing the initiation and development of ARs, which will be applicable to crop agriculture in extreme wind climates.

Key words: Adventitious root, heat stress, protein quality control, thermotolerance, thigmomorphogenesis, wind

Student Number: 2014-22389

CONTENTS

LIST OF FIGURES

LIST OF TABLES

ABBREVIATIONS

AC	Acclimation
ABA	Abscisic acid
AR	Adventitious root
ARL1	ADVENTITIOUS ROOTLESS 1
APX	Ascorbate peroxidase
BiFC	Bimolecular fluorescence complementation
CaMV	Cauliflower mosaic virus
CAB2	CHLOROPHYLL A/B-BINDING PROTEIN 2
CAT3	CATALASE 3
CCR2	COLD, CIRCADIAN RHYTHM, AND RNA BIDING 2
CHIP	CARBOXYL TERMINUS OF HSC70-INTERACTING PROTEIN
DIC	Differential interference contrast
DREB	Dehydration-responsive element binding
GA	Gibberellic acid
GFP	Green fluorescent protein
GI	GIGANTEA

HSF	Heat shock transcription factor
HSP	Heat shock protein
HXK1	HEXOKINASE 1
IAA	Indole-3-acetic acid
IgG	Immunoglobulin G
IP	Immunoprecipitation
JA	Jasmonic acid
LBD	LATERAL ORGAN BOUNDARIES DOMAIN
LC-MS/MS	Liquid chromatography tandem-mass spectrometry
LD	Long day
LHY	LATE ELONGATED HYPOCOTYL 1
MS	Murashige and Skoog
NBR1	NEIGHBOR OF BRCA1 GENE 1
NC	Nonacclimation
NPA	*N*-1-Naphthylphthalamic acid
PIN	PIN-FORMED
PRR5	PSEUDO-RESPONSE REGULATOR 5
RT-PCR	Reverse transcription polymerase chain reaction
RT-qPCR	Quantitative real-time PCR
SD	Standard deviation

SEM	Standard error of the mean
TOC1	TIMING OF CAB EXPRESSION 1
TUB	TUBULIN
WOX	WUSCHEL RELATED HOMEOBOX
YFP	Yellow fluorescent protein
ZTL	ZEITLUPE

CHAPTER 1

ZEITLUPE contributes to a thermoresponsive protein quality control system in *Arabidopsis*

INTRODUCTION

Protein misfolding occurs not only during normal cellular folding processes but also under environmental and oxidative stress conditions. Accumulation of misfolded proteins leads to the formation of insoluble aggregates, which are toxic to protein homeostasis and cellular integrity in eukaryotes (McClellan et al., 2005). Versatile protein quality control mechanisms have evolved to deal with misfolded proteins and insoluble protein aggregates by either facilitating their refolding into native conformations or directing their degradation via diverse ubiquitin-proteasome pathways (Finka and Goloubinoff, 2013).

Controlled protein degradation via the ubiquitin-proteasome pathway is initiated when molecular chaperones, such as heat shock protein 70 (HSP70) and HSP90, fail to refold misfolded proteins into their native state (McClellan et al., 2005; Finka and Goloubinoff, 2013). The molecular chaperones recognize the hydrophobic parts of misfolded proteins and recruit distinct ubiquitin ligase enzymes to the protein aggregates, forming ubiquitin-proteasome apparatuses that determine which parts of the aggregates are to be removed (McClellan et al., 2005). For example, the carboxy terminal domain of Hsc70-interacting protein (CHIP)

plays an important role in eliminating cytosolic protein aggregates by selectively ubiquitinating HSP70-associated misfolded proteins in animals and plants (Zhou et al., 2014; Lee et al., 2009). It is also known that the Cullin5 E3 ubiquitin ligase triggers polyubiquitination-mediated proteasomal degradation of HSP90 clients in animal cells (Samant et al., 2014).

HSP90 is a key molecular chaperone that is abundant and highly conserved in eukaryotes (McClellan et al., 2005; Krishna and Gloor, 2001). It plays essential roles in signal transduction pathways and cell cycle control by enhancing cell viability under stressful conditions (Krishna and Gloor, 2001; Finka et al., 2015). In *Arabidopsis*, there are seven HSP90 members that are localized in distinct subcellular compartments (Krishna and Gloor, 2001). They are functionally associated with the maturation and stabilization processes of numerous regulatory proteins functioning in diverse signaling networks. It has been shown that HSP90 interacts with cochaperone SGT1, stabilizing the immune-sensing nucleotide-binding domain and leucine-rich repeat proteins (Shirasu, 2009). HSP90 also plays a role in buffering genetic variation and ensuring developmental stability (Sangster et al., 2008; Sangster and Queitsch, 2005).

The HSP90 molecular chaperone also participates in cellular responses to environmental stress and its roles in thermal adaptive responses are best understood. HSP90 prevents cellular damage by facilitating the refolding of misfolded proteins

at high temperatures and removing heat-induced protein aggregates in metazoan species and yeast (Borkovich et al., 1989; Dickey et al., 2007). Accumulating evidence also supports that plant HSP90 proteins mediate various aspects of heat stress responses (Xu et al., 2012). It is notable that high-temperature stress influences virtually all facets of plant growth and development, covering seed germination to flowering (Bita and Gerats, 2013). HSP90 also affects plant environmental performance and clock function (Filichkin et al., 2015), necessitating that the interactions of HSP90 with distinct E3 ubiquitin ligases during plant environmental adaptation are more complicated than previously thought.

Recently, it has been shown that HSP90 acts as a molecular chaperone for the F-box protein ZEITLUPE (ZTL) in *Arabidopsis* (Kim et al., 2011). The ZTL acts as an evening-phased clock component that mediates proteasomal degradation of the clock components TIMING OF CAB EXPRESSION 1 (TOC1) and PSEUDO-RESPONSE REGULATOR 5 (PRR5) (Más et al., 2003; Kiba et al., 2007). The levels of ZTL protein oscillate in a circadian manner. It has been reported that HSP90, in conjunction with GIGANTEA (GI), stabilizes ZTL in the afternoon (Kim et al., 2011). ZTL is unique among the known HSP90 clients in that the molecular chaperone stabilizes and facilitates the correct folding of the heat-denatured client (Cha et al., 2015). Together with the pivotal roles of HSP90 in

thermal responses, these observations raise the possibility that the ZTL-HSP90 complex underlies the thermostable nature of the circadian clock in plants.

In this work, I demonstrated that ZTL, together with its interacting molecular chaperone HSP90, enhances the thermotolerance of plant growth by promoting polyubiquitination of misfolded proteins at high temperatures. Whereas ZTL-HSP90 protein complexes were dispersed in the cytoplasm at normal temperatures, the protein complexes were associated with insoluble protein aggregates in the cytoplasm at high temperatures. Interestingly, circadian rhythms were more rapidly dampened in the ZTL-defective mutant compared to those in control plants under heat stress conditions. Together, I propose that the ZTL-mediated polyubiquitination of protein aggregates is essential for thermotolerance and provides the means for sustaining robust clock function under stressful high-temperature conditions.

MATERIALS AND METHODS

Plant materials and growth conditions

All *Arabidopsis thaliana* lines used were in the Columbia (Col-0) background. Sterilized seeds were stratified at 4ºC in darkness for 3 d and allowed to germinate on ½ X Murashige and Skoog-agar plates (hereafter referred to as MS-agar plates) at 23ºC under long days (LDs, 16-h light and 8-h dark). White light illumination (120 µmol photons $m^{-2}s^{-1}$) was provided by fluorescent FLR40D/A tubes (Osram).

The T-DNA insertional knockout mutants, *prr7-11* and *ztl-105,* have been described previously (Yamamoto et al., 2003; Martin-Tryon et al., 2007). A MYC-coding sequence was fused in-frame to the 3' end of the ZTL-coding sequence, and the gene fusion was subcloned into the binary pBA002 vector under the control of either the Cauliflower Mosaic Virus (CaMV) 35S promoter or the endogenous *ZTL* gene promoter, consisting of ~1.8 kbp sequence region upstream of the translational start site (Baudry et al., 2010). The expression constructs were transformed into Col-0 plants or *ztl-105* mutant, resulting in $35S_{pro}$*:ZTL-MYC* or ZTL_{pro}*:ZTL-MYC ztl-105*, respectively. The ZTL-coding sequence was also subcloned into the binary pB2GW7 vector under the control of the CaMV 35S promoter, and the expression construct was transformed into Col-0 plants. The

ZTL-overexpressing plants were used in thermotolerance assays.

Transcript abundance measurement

Total RNA samples were extracted from ten-day-old seedlings grown on MS-agar plates and pretreated with RNase-free DNase to eliminate genomic DNA contamination before RT-qPCR. RT-qPCR reactions were carried out in 96-well blocks with an Applied Biosystems 7500 Real-Time PCR System (Foster City) using the SYBR Green I master mix in a volume of 20 μL. PCR primers were designed using the Primer Express Software installed into the system and listed in Table 1. Individual PCR reactions were set up as follows: 10 min at 95°C, followed by 35 ~ 40 cycles of 15 s at 95°C for denaturation and 1 min at 60°C for annealing and polymerization and an additional round of 1 min at 65°C at the end of the thermal cycles for completion of PCR reactions. An *eIF4A* gene (At3g13920) was included in the reactions as internal control to normalize the variations in the amounts of cDNA used (Gutierrez et al., 2008).

All RT-qPCR reactions were performed using three independent samples prepared from different plants grown under identical conditions. The comparative $\Delta\Delta C_T$ method was employed to evaluate relative quantities of individual amplified products in the samples. The threshold cycle C_T was automatically determined for each reaction by the system set with default parameters. The specificity of the RT-

qPCR reactions was determined by melt curve analysis of the amplified products using the standard method installed into the system.

Thermotolerance assay

The assays were performed essentially as described previously (Yoo et al., 2006), but with some modifications. Seven-day-old seedlings grown on MS-agar plates were exposed to 40°C for 4.5 h in darkness and allowed to recover at 23°C for 5 d under LDs. Survival of heat-treated seedlings was decided based on the existence of newly developing leaves. For heat acclimation assays, seedlings were exposed to 37°C for 1 h and then incubated at 23°C for 2 h before exposure to 45°C for 1.5 h in darkness. The heat-treated seedlings were then allowed to recover at 23°C for 5 d under LDs.

Measurement of chlorophyll contents

Measurement of chlorophyll contents were performed as described previously (Lee et al., 2012). Briefly, plant materials were ground in liquid nitrogen, and chlorophylls were extracted with N,N-dimethylformamide. The extract was incubated at 4°C for 1 h in complete darkness. Chlorophyll contents were assayed by measuring absorbance at 652, 665, and 750 nm using a diode array spectrophotometer (WPA Biowave).

Detection of polyubiquitinated proteins

Eight-day-old seedlings grown on MS-agar plates were transferred to MS liquid culture for 1 d under LDs before exposure to 40ºC. Plant materials were ground in liquid nitrogen, and total proteins were eluted with 2 X SDS-PAGE loading buffer (100 mM Tris-Cl, pH 6.8, 4% sodium dodecyl sulfate, 0.2% bromophenol blue, 20% glycerol, and 200 mM DTT) and boiled for 10 min. The boiled extract was clarified by centrifugation at 23ºC for 10 min at 12,000 X *g*. Fifteen μL of the supernatant was loaded onto a 6% SDS-PAGE gel and then transferred onto PVDF membrane (catalog no. IPVH00010; Millipore). Polyubiquitinated proteins were detected immunologically using a monoclonal anti-ubiquitin antibody produced in mouse (catalog no. sc-8017; Santa Cruz Biotechnology). For the secondary antibody, a goat anti-mouse IgG-horseradish peroxidase (HRP) (catalog no. sc-2005; Santa Cruz Biotechnology) was used. After incubation with the secondary antibody, HRP-conjugated proteins were visualized using the West Save Up system (catalog no. LF-QC0101; Abfrontier). The relative intensities of polyubiquitinated proteins were quantitated using the ImageJ software (https://imagej.nih.gov/ij/).

Fractionation of soluble and insoluble proteins

The fractionation was performed as described previously (Coll et al., 2014). Plant

materials were ground in liquid nitrogen and suspended in buffer B containing apyrase (catalog no. A6535; Sigma-Aldrich) and/or MG132. The protein extract was passed through a cell strainer having pore sizes of 70 μm (Fisher Scientific), and the solution was centrifuged sequentially at 2,000 X *g* at 10 min followed by centrifugation at 3,000 X *g* for 10 min at 4ºC. The supernatant was centrifuged again at 16,000 X *g* at 4ºC for 90 min. The supernatant and the pellet correspond to soluble and insoluble fractions, respectively. The pellet was washed three times with fresh buffer B supplemented with 2% Nonidet p-40, each by centrifugation at 16,000 X *g* for 30 min. The pellet was resuspended in fresh buffer B and sonicated using an ultrasonic cleaner (SaeHan ultrasonic). The solutions were mixed with 5 X SDS-PAGE loading buffer and boiled for 10 min.

The samples were analyzed on 6% and 10% SDS-PAGE gels. The 6% gel was either Coomassie blue-stained or subjected to immunoblotting analysis using an anti-ubiquitin antibody (Santa Cruz Biotechnology). A modified version of Coomassie blue staining was employed to detect the fractionated proteins with improved sensitivity (Wang et al., 2007). The 10% gel was blotted onto PVDF membrane, and HSP90.1, tubulin, and ZTL-MYC proteins were detected immunologically using a polyclonal anti-HSP90.1 antibody produced in rabbit (catalog no. AS08 346; Agrisera), a monoclonal anti-tubulin antibody produced in mouse (catalog no. T9026; Sigma-Aldrich), and a monoclonal anti-MYC antibody

produced in mouse (catalog no. 05-724; Millipore), respectively. For the secondary antibodies, a goat anti-mouse IgG-HRP (Santa Cruz Biotechnology) and a goat anti-rabbit IgG-HRP (catalog no. sc-2030; Santa Cruz Biotechnology) were used.

Mass spectrometry of insoluble proteins was performed at the National Instrumentation Center for Environmental Management, Seoul National University, using the nano high-resolution LC-MS/MS spectrometer (Thermo Scientific). Among the identified proteins, HXK1 proteins were immunologically detected using a polyclonal anti-HXK1 antibody produced in rabbit (catalog no. AS12 2601; Agrisera).

Protein stability assay

To examine the stability of ZTL proteins at high temperatures, the *35S$_{pro}$:ZTL-MYC* transgenic plants were grown on MS-agar plates for 10 d under LDs. After incubation at 40^{o}C in darkness, whole plants were harvested for the extraction of total proteins. ZTL proteins were detected immunologically using an anti-MYC antibody (Millipore).

Bimolecular fluorescence complementation (BiFC) assay

The assays were conducted as described previously (Seo et al., 2012). Full-size ZTL- and HSP90.1-coding sequences were fused in-frame to the 3' end of a gene

sequence encoding the N-terminal half of enhanced YFP in the pSATN-nEYFP-C1 vector (E3081) or to the 3' end of a gene sequence encoding the C-terminal half of enhanced YFP in the pSATN-cEYFP-C1 vector (E3082). The expression constructs were cotransformed into *Arabidopsis* mesophyll protoplasts by the PEG-calcium transfection method. Transformed protoplasts were incubated for 16 h under constant light, and reconstitution of YFP fluorescence was monitored by fluorescence microscopy using a Zeiss LSM510 confocal microscope (Carl Zeiss) with the following filter setup: 514 nm for excitation, 535-590 nm for YFP, 690-730 nm for autofluorescence.

Coimmunoprecipitation assay

Plants were grown on MS-agar plates for 9 d at 23°C. After incubation at 40ºC in darkness for 2 h, whole plants were harvested for the extraction of total proteins. Plant materials were ground in liquid nitrogen, and proteins were extracted in coimmunoprecipitation buffer (50 mM Tris-Cl pH 7.4, 500 mM NaCl, 10% glycerol, 5 mM EDTA, 1% Triton-X-100, 1% Nonidet P-40) containing protease inhibitor cocktail tablets (catalog no. 11836153001; Sigma-Aldrich). Five % of the extracts was used as input control. The protein extracts were incubated with 20 μL polyclonal anti-c-Myc agarose affinity gel antibody produced in rabbit (catalog no. A7470; Sigma-Aldrich) for 1 h at 4ºC. The beads were then washed five times with

fresh coimmunoprecipitation buffer. To elute proteins, 40 μL of 2 X SDS loading buffer was added to the beads and boiled for 10 min. Twenty % of the eluted proteins were used as IP control. An anti-MYC (Millipore) and an anti-HSP90.1 (Agrisera) antibodies were used for the detection of ZTL-MYC and HSP90.1, respectively.

Circadian rhythm measurement

One-week-old plants grown on MS-agar plates under LDs were exposed to 23ºC, 28ºC, 35ºC, or 42ºC for up to 3 d under constant light conditions. Whole plant materials were harvested at appropriate ZT points for total RNA extraction. Gene transcript levels were examined by RT-qPCR. The period and relative amplitude error of rhythmicity were calculated using the BioDare2 software (https://biodare2.ed.ac.uk/welcome).

Primers	Usage	Sequences
eIF4a-F	RT-qPCR	5′-TGACCACACAGTCTCTGCAA
eIF4a-R	RT-qPCR	5′-ACCAGGGAGACTTGTTGGAC
DREB2A-F	RT-qPCR	5′-ATGGTCCTTTGGCTCGTCTT
DREB2A-R	RT-qPCR	5′-TCCACCGGAGAAGGGTTTAG
DREB2B-F	RT-qPCR	5′-CGGTTCATTGGCTCGTCTTA
DREB2B-R	RT-qPCR	5′-ACCGCCTTATTTTCAACCGT
APX1-F	RT-qPCR	5′-CCAACCGTGAGCGAAGATTA
APX1-R	RT-qPCR	5′-CGTCAAACCTCATTGTTCCG
APX2-F	RT-qPCR	5′-TGCATTGTCTGGTGGACACA
APX2-R	RT-qPCR	5′-GAAGAGCCTTGTCGGTTGGT
HSFA1a-F	RT-qPCR	5′-CCCCTTTCCTTAGCAAGACG
HSFA1a-R	RT-qPCR	5′-TAACTGGCGAACAAAGCTGG
HSFA1b-F	RT-qPCR	5′-GTGTCGAGGTGGGGAAGTTT
HSFA1b-R	RT-qPCR	5′-TTTGTTGTTGCCTTTGCTCC
HSFA1d-F	RT-qPCR	5′-GGATTCAACACCAGTGGACAATG
HSFA1d-R	RT-qPCR	5′-AGGAGACCCATCTGTTGAGTCAG
HSFA2-F	RT-qPCR	5′-GGGGAGGTTGAGAGGTTGAA
HSFA2-R	RT-qPCR	5′-TTGGCAAGGAACGTCATCAT
HSP60-F	RT-qPCR	5′-CAGAATGAGCTGGAGCAGGA
HSP60-R	RT-qPCR	5′-TGGGACCCATGGTGACTTTA
HSP70-F	RT-qPCR	5′-TGAGGCAGATGAGTTCGAGG
HSP70-R	RT-qPCR	5′-CTCCTGCACCACCCATATCA
HSP90-F	RT-qPCR	5′-TTTGGTGTTGGTTTCTACTCTGCTTA
HSP90-R	RT-qPCR	5′-TCGTTCTGACCTTCCTTCATCCTTGT
HSP101-F	RT-qPCR	5′-GGCTTGACGAGATTGTGGTG
HSP101-R	RT-qPCR	5′-CGGGTCATAACTCTCTGCCA
ZTL-F	RT-qPCR	5′-ACGTTGCAGTTAACCTCCCTG
ZTL-R	RT-qPCR	5′-TTACGTGAGATAGCTCGCTAGTGA
TOC1-F	RT-qPCR	5′-TCTTCGCAGAATCCCTGTGAT
TOC1-R	RT-qPCR	5′-GCTGCACCTAGCTTCAAGCA
CAT3-F	RT-qPCR	5′-TTCCCACCCCTACAAACTCC
CAT3-R	RT-qPCR	5′-CCTGTCTTGCCTGTCTGGTG
CCR2-F	RT-qPCR	5′-GCTCTTGAGACTGCCTTCGCTC
CCR2-R	RT-qPCR	5′-CTCGTTAACAGTGATGCTACGG
ZTL ($35S_{pro}$)-F	Cloning	5′-AAAAAGCAGGCTCCATGGAGTGGGACAGTGGTTC
ZTL ($35S_{pro}$)-R	Cloning	5′-AGAAAGCTGGGTATTACGTGAGATAGCTCGCTAGTG
ZTL-MYC($35S_{pro}$)-F	Cloning	5′-CCGCTCGAGATGGAGTGGGACAGTGGTTC
ZTL-MYC($35S_{pro}$)-R	Cloning	5′-CAGGACGTCTGCGTGAGATAGCTCGCTAGTGATA
ZTL-MYC(ZTL_{pro})-F	Cloning	5′-CGGGATCCGCATGGAGTGGGACAGTGGTTC
ZTL-MYC(ZTL_{pro})-R	Cloning	5′-CCGCTCGAGACGTGAGATAGCTCGCTAGTGATA
ZTL promoter-F	Cloning	5′-CATGCCATGGgaacgaggtgaagaatgtcg
ZTL promoter-R	Cloning	5′-CAGCCTAGGGAAAATTCAAATAGTTACCAGACTG
ZTL BiFC-F	Cloning	5′-CCGCTCGAGCTATGGAGTGGGACAGTGGTTC
ZTL BiFC-R	Cloning	5′-CGGGATCCTTACGTGAGATAGCTCGCTAGTG
HSP90.1 BiFC-F	Cloning	5′-CCGCTCGAGCTATGGCGGATGTTCAGATGG
HSP90.1 BiFC-R	Cloning	5′-CGGGATCCTTAGTCGACTTCCTCCATCTTGC

Table 1. Primers used in CHAPTER 1.

F and R indicate forward and reverse primers, respectively. The primers were designed according to the rules suggested by the Primer3 software (version 0.4.0, http://primer3.sourceforge.net/releases.php) so that they have calculated melting temperatures in a range of 50 - 65 ^{o}C.

RESULTS

The *ztl-105* mutant exhibits reduced thermotolerance

On the basis of HSP90-mediated stabilization of ZTL proteins (Kim et al., 2011; Cha et al., 2015; Cha et al., 2017), I hypothesized that ZTL would be involved in the heat stress response. To examine this hypothesis, I first examined the thermosensitivity of the ZTL-defective mutant and *ZTL*-overexpressing plants (Figure 1). As ZTL protein abundance is under diurnal control (Kim et al., 2003), plants were treated with high temperatures at a specific time, the midpoint of the day under long days. It was found that the *ztl-105* mutant exhibited significantly reduced thermotolerance, while *ZTL*-overexpressing plants exhibited enhanced thermotolerance compared with Col-0 plants (Figure 2A and Figure 2B). Consistent with the altered thermal responses, chlorophyll contents were accordingly lower in the *ztl-105* mutant but higher in the *ZTL*-overexpressing plants (Figure 2C), supporting that ZTL is involved in plant thermotolerance.

To investigate whether thermal responses vary over the day, I performed thermotolerance assays at different time points. At the end of the day, the reduced thermotolerance of the *ztl-105* mutant was still evident (Figure 3). In contrast, at the end of the night, there were no significant differences in thermotolerance between Col-0 plants and the *ztl-105* mutant, indicating that the ZTL-mediated

thermal responses fluctuate throughout the diurnal cycle.

To verify that the reduced thermotolerance of the *ztl-105* mutant was caused by the loss-of-function mutation, the mutant was complemented with a genomic *ZTL* gene, whose expression was driven by the endogenous gene promoter. The reduced thermotolerance of the *ztl-105* mutant was efficiently rescued in the complemented plants (Figure 4), indicating that ZTL is functionally associated with the thermoresponsive phenotype of the mutant.

The *ztl-105* mutant exhibits a longer circadian period than Col-0 plants (Martin-Tryon et al., 2007). A question remained on whether the thermal response of the mutant is associated with its longer circadian period. I examined the thermal responsiveness of another long-period mutant *prr7-11* (Farré et al., 2005). The basal thermotolerance of the *prr7-11* mutant was not discernibly different from Col-0 plants (Figure 5) indicating that the reduced thermotolerance phenotype of the *ztl-105* mutant is independent of circadian periodicity.

I next examined whether ZTL is associated with heat acclimation. Plants were pretreated at 37^{o}C before exposure to higher temperatures. Measurements of survival rates and chlorophyll contents revealed that acquired thermotolerance was reduced in the *ztl-105* mutant (Figure 6) but enhanced in *ZTL*-overexpressing plants (Figure 7), indicating that ZTL is associated with both basal and acquired thermotolerance responses.

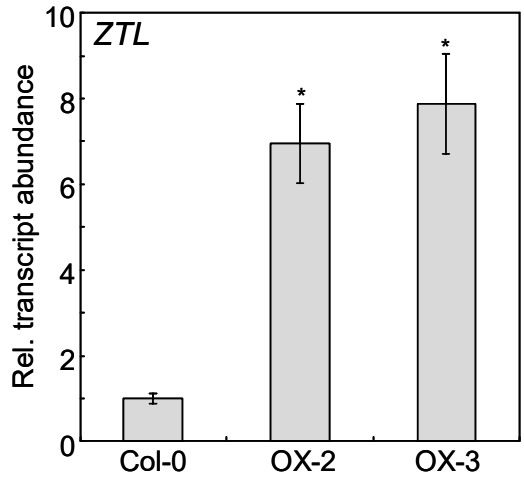

Figure 1. Molecular validation of *ZTL*-overexpressing plants.

A ZTL-coding sequence was overexpressed driven by the Cauliflower Mosaic Virus (CaMV) 35S promoter in Col-0 plants. Multiple transgenic lines were obtained, and overexpression of the transgene was verified. Two representative overexpressing lines (OX-2 and OX-3) were chosen for further analysis. One-week-old plants grown on MS-agar plates were used for total RNA extraction. Gene transcript levels were examined by reverse transcription-mediated quantitative real-time PCR (RT-qPCR). Biological triplicates were averaged and statistically analyzed (*t*-test, * $P < 0.01$). Bars indicate standard error of the mean (SEM).

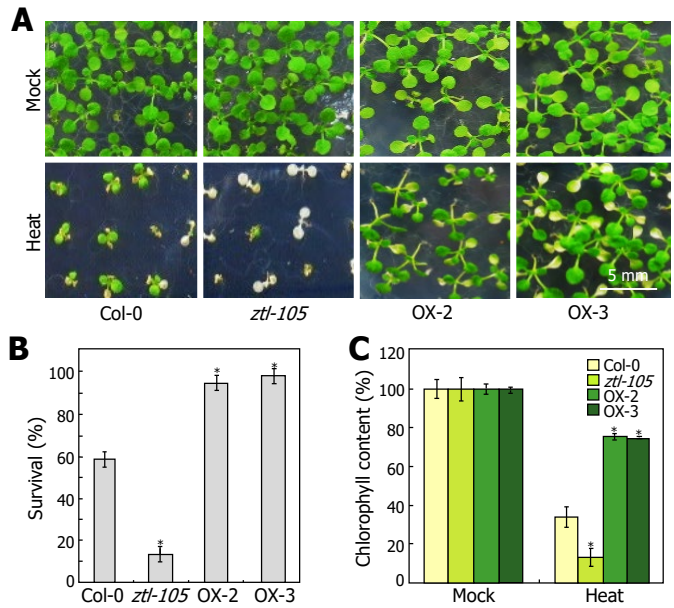

Figure 2. Reduced basal thermotolerance in *ztl-105* mutant.

One-week-old plants grown on MS-agar plates were exposed to 40^{o}C at the midpoint of the day for 4.5 h in darkness and allowed to recover at 23^{o}C for 5 d **(A)**. Two measurements of survival rates **(B)** and chlorophyll contents **(C)**, each consisting of 30 plants, were averaged and statistically analyzed (*t*-test, **P* < 0.01). Bars indicate standard error of the mean (SEM).

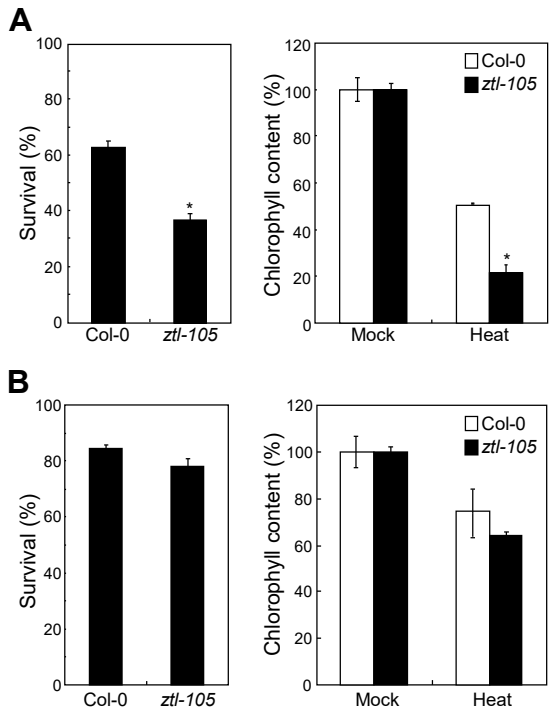

Figure 3. Thermal responses depend on diurnal cycles.

One-week-old plants grown on MS-agar plates were exposed to 40^{o}C for 7.5 h at the end of the day **(A)** or for 3.5 h at the end of the night **(B)** in darkness and allowed to recover at 23^{o}C for 5 days. Two measurements of survival rates and chlorophyll contents, each consisting of 30 plants, were averaged and statistically analyzed (*t*-test, **P* < 0.01). Bars indicate SEM.

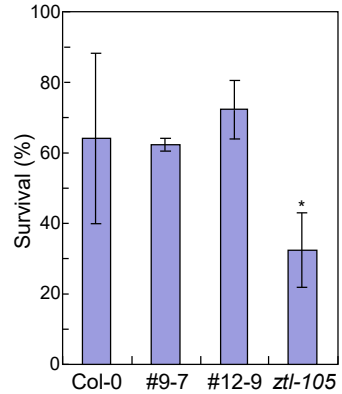

Figure 4. Complementation of *ztl-105* mutant.

A *ZTL-MYC* fusion, in which a MYC-coding sequence was fused in-frame to the 3‘ end of the ZTL-coding sequence, was expressed driven by the endogenous gene promoter consisting of ~1.8-kb region upstream of the translation start site in *ztl-105* mutant (Baudry et al., 2010), resulting in ZTL_{pro}*:ZTL-MYC ztl-105*. One-week-old plants grown on MS-agar plates were exposed to 40^{o}C for 3.5 h and allowed to recover at 23^{o}C for 5 days (left panel). Two measurements of survival rates, each consisting of 30 seedlings, were averaged and statistically analyzed using Student *t*-test (*$P < 0.01$) (right panel). Bars indicate SEM.

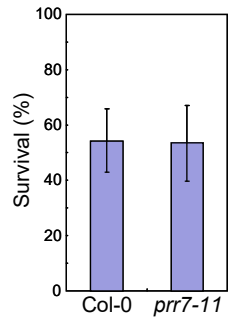

Figure 5. Thermal responses are independent of long periodicity.

One-week-old plants grown on MS-agar plates were exposed to 40°C for 4.5 h at the midpoint of the day and allowed to recover at 23°C for 5 days (left panel). Two measurements of survival rates, each consisting of 30 seedlings, were averaged and statistically analyzed using Student *t*-test (*$P < 0.01$) (right panel). Bars indicate SEM.

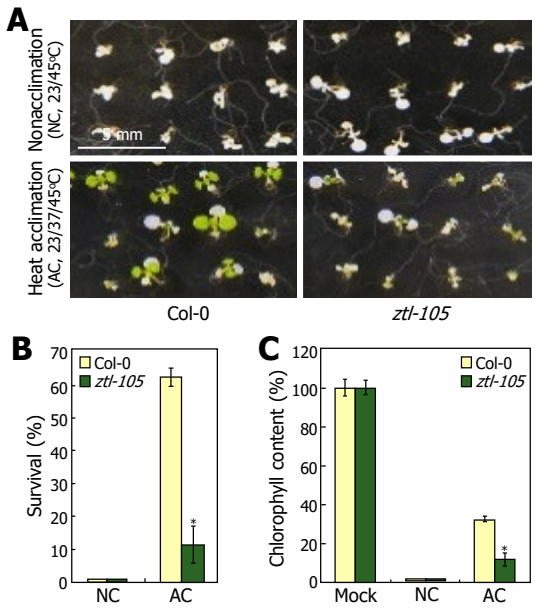

Figure 6. Reduced acquired thermotolerance in *ztl-105* mutant.

One-week-old plants grown on MS-agar plates were pre-incubated at 37°C for 1 h in darkness and subsequently at 23°C for 2 h before exposure to 45°C for 1.5 h in darkness. The heat-treated plants were allowed to recover at 23°C for 5 d **(A)**. Survival rates **(B)** and chlorophyll contents **(C)** were measured as described in Figure 1. NC, nonacclimation. AC, heat acclimation.

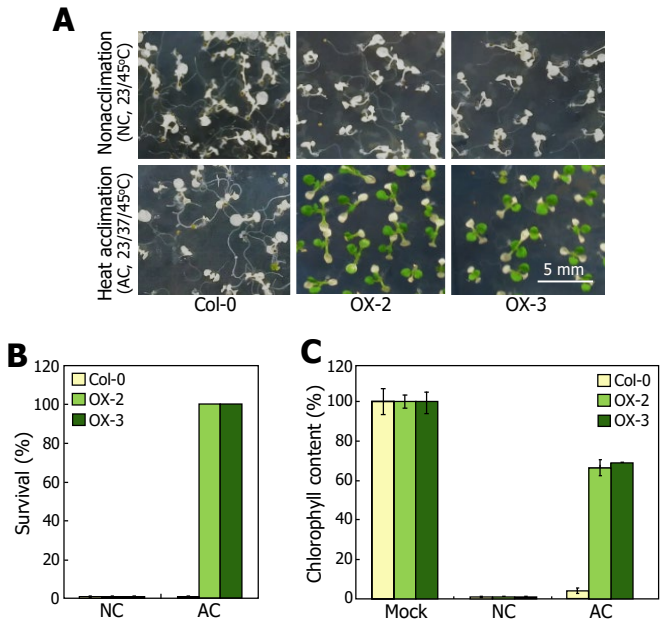

Figure 7. Enhanced acquired thermotolerance in *ZTL*-overexpressing plants.

One-week-old plants grown on MS-agar plates were pre-incubated at 37°C for 1 h in darkness and subsequently at 23°C for 2 h before exposure to 45°C for 3 h in darkness. The heat-treated plants were allowed to recover at 23°C for 5 d **(A)**. Two measurements of survival rates **(B)** and chlorophyll contents **(C)** were measured, as described in Figure 1.

Polyubiquitination is suppressed in the *ztl-105* mutant under heat stress

A large set of HSPs and heat shock factors (HSFs) is known to mediate heat stress response and signaling in *Arabidopsis* (von Koskull-Döring et al., 2007). I investigated whether ZTL-mediated thermotolerance is functionally linked with known HSPs and HSFs. Measurements of transcript abundance by reverse transcription-mediated quantitative real-time PCR (RT-qPCR) showed that the relative transcript levels of *HSP* and *HSF* genes were similar in Col-0 plants and the *ztl-105* mutant at high temperatures (Figure 8A). The dehydration-responsive element binding (DREB) transcription factors play a regulatory role in drought and heat stress responses (Lata and Prasad, 2011). Ascorbate peroxidase (APX) is an antioxidant enzyme functioning in a broad spectrum of abiotic stress responses, including heat stress, by detoxifying hydrogen peroxide (Panchuk et al., 2002). I found that expression of the *DREB* and *APX* genes was also unaffected by the *ztl-105* mutation (Figure 8B). These observations indicate that ZTL-mediated thermotolerance occurs independently of known heat stress signaling pathways, at least at the transcriptional level.

Under heat stress, misfolded proteins that are excluded from the refolding process undergo polyubiquitination and are subsequently degraded through the ubiquitin-proteasome pathways to maintain protein homeostasis (McClellan et al., 2005; Finka and Goloubinoff, 2013). I found that the *ztl-105*

mutant is susceptible to high temperatures. Therefore, I investigated whether the ZTL enzyme mediates the heat-induced polyubiquitination process.

Plants were exposed to 40ºC, and polyubiquitinated proteins were immunologically detected in total protein extracts. It was found that polyubiquitination was not altered in either Col-0 plants or the *ztl-105* mutant at 23ºC in darkness (Figure 9A). Notably, following exposure to heat stress, the level of polyubiquitination was rapidly elevated within one hour in Col-0 plants (Figure 9B). However, the rate of elevation was detectably reduced in the *ztl-105* mutant. In addition, the differential effects of heat stress on polyubiquitination were also observed in light-treated plants (Figure 9C), indicating that ZTL helps to increase heat-induced polyubiquitination regardless of light. Meanwhile, the reduced polyubiquitination was recovered in the *ztl-105* complemented lines (Figure 10), further supporting the role of ZTL in heat-induced polyubiquitination.

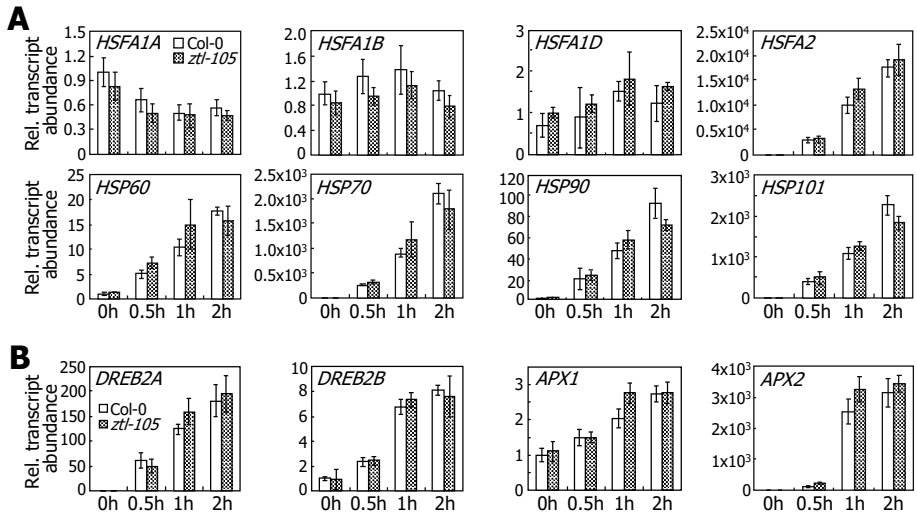

Figure 8. Quantification of the transcript levels of heat stress genes in *ztl-105* mutant.

Ten-day-old plants grown on MS-agar plates were exposed to 40^{o}C at the midpoint of the day for the indicated time durations before harvesting whole plants for total RNA extraction. Transcript levels of *HSF* and *HSP* **(A)** and *DREB* and *APX* **(B)** genes were examined by RT-qPCR. Biological triplicates were averaged (*t*-test, $P < 0.01$). Bars indicate SEM. Note that there are no significant differences in the transcript levels of the tested genes.

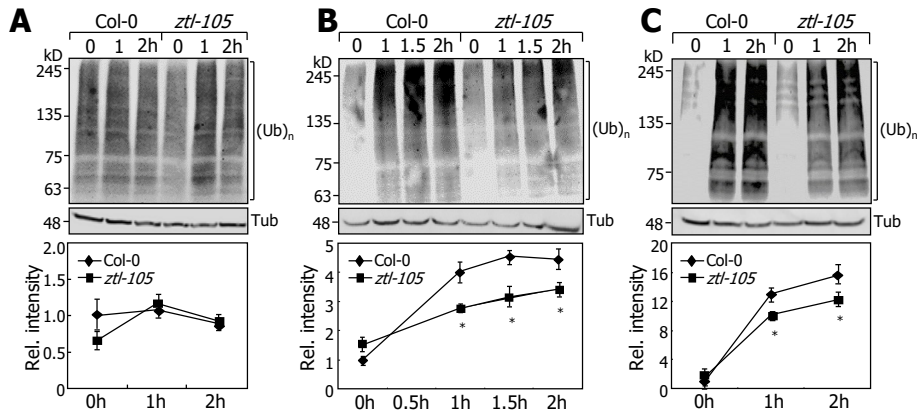

Figure 9. Heat-induced polyubiquitination is reduced in *ztl-105* mutant.

Eight-day-old plants grown on MS-agar plates were transferred to MS liquid culture at 23°C for 1 d. They were then exposed to either 23°C **(A)** or 40°C **(B)** in darkness for the indicated time durations. They were also exposed to 40°C in the light **(C)**. Total proteins were extracted from whole plants, and polyubiquitinated proteins were detected immunologically using an anti-ubiquitin (Ub) antibody. Tubulin (Tub) proteins were also immunologically detected for loading control. For each treatment, three blots were quantitated using the ImageJ software (http://rsb.info.nih.gov/ij/) and averaged (*t*-test, $*P < 0.01$). Bars indicate standard deviation (SD).

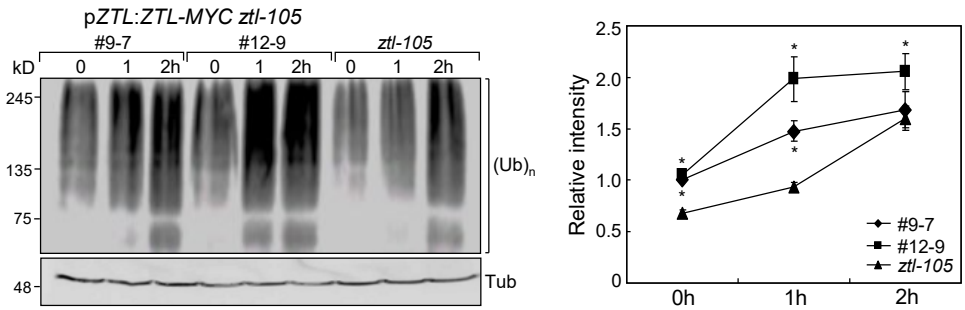

Figure 10. Levels of polyubiquitinated proteins in *ztl-105* complemented lines.

Eight-day-old plants grown on MS-agar plates were transferred to MS liquid culture at 23°C for 1 day. They were then exposed to 40°C in darkness for up to 2 h before extracting total proteins. Polyubiquitinated proteins were detected immunologically using an anti-ubiquitin (Ub) antibody (left panel). Tubulin (Tub) proteins were immunologically detected in a similar manner for loading control. Three blots were quantitated using the ImageJ software and averaged (right panel). Bars indicate standard deviation (*t*-test, $*P < 0.01$, difference from *ztl-105*). Note that the reduction of protein polyubiquitination in the mutant was rescued in the complemented lines.

Accumulation of protein aggregates is elevated in the *ztl-105* mutant under heat stress

Misfolded proteins formed under unfavorable stress conditions are either refolded into their native conformations or deposited as insoluble aggregates, which are subsequently removed by the ubiquitin-proteasome pathways (McClellan et al., 2005; Finka and Goloubinoff, 2013). As a result, reduction of polyubiquitination often accompanies accumulation of insoluble aggregates. I found that ZTL enhances protein polyubiquitination under heat stress, suggesting that protein aggregates would accumulate in the *ztl-105* mutant.

Total proteins were extracted from plants exposed to 40^{o}C in darkness and fractionated into soluble and insoluble forms. It was found that the levels of insoluble protein aggregates were detectably elevated in the heat-treated *ztl-105* mutant (Figure 11A), which is certainly related to the reduced polyubiquitination in the mutant at high temperatures (Figures 9B, 9C, and 11B). In contrast, the levels of insoluble protein aggregates were reduced but protein polyubiquitination was elevated in *ZTL*-overexpressing plants (Figures 12), indicating that ZTL is important for clearing protein aggregates.

The molecular chaperone HSP90 is an interacting partner of ZTL (Kim et al., 2011), which mediates the polyubiquitination process of cellular proteins at high temperatures. It was notable that whereas most HSP90 proteins were present

in soluble fractions under normal temperature conditions, it was detected in both the soluble and insoluble fractions at high temperatures (Figure 11A). These observations support that ZTL and its interacting partner HSP90 constitute a part of a heat-inducible protein quality control system, which is able to clear insoluble protein aggregates through the ubiquitin-proteasome pathways.

The next question was how heat stress affects ZTL function in the quality control of cellular proteins. It was found that *ZTL* transcription was only slightly elevated at high temperatures (Figure 13A). The protein levels of ZTL were also unaltered by heat stress (Figure 13B). Therefore, it is evident that heat stress does not affect ZTL function at the levels of gene transcription and protein production and stability.

It is known that subcellular localization of ubiquitin ligases underlies the ubiquitin-dependent degradation of target proteins (Huett et al., 2012; Heck et al., 2010). I therefore examined the dynamic association of ZTL with protein aggregates at high temperatures. Transgenic plants overproducing a ZTL-MYC fusion were heat-treated, and total proteins were separated into soluble and insoluble fractions. Interestingly, both ZTL proteins and polyubiquitinated proteins cofractionated in insoluble fractions at 40^{o}C (Figure 13C), indicating that ZTL proteins are shuttled to protein aggregates under heat stress, possibly in conjunction with HSP90.

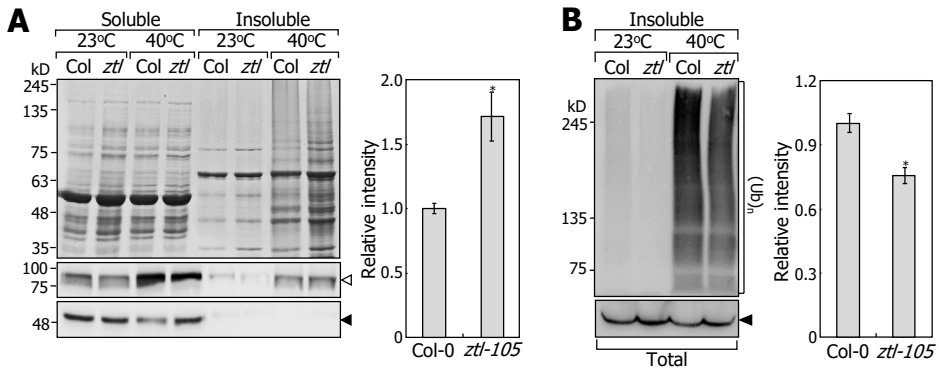

Figure 11. Levels of protein aggregates in *ztl-105* mutant.

Eight-day-old plants grown on MS-agar plates were transferred to MS liquid culture at 23°C for 1 d. At the midpoint of the day, they were then exposed to 40°C in darkness for 2 h before preparing soluble and insoluble fractions. In **(A)**, protein blots were stained with Coomassie blue (uppermost panel), and HSP90 and Tub were immunologically detected (lower panels). Black and white arrowheads indicate Tub and HSP90, respectively. Relative levels of accumulated aggregates at high temperatures were quantitated using the ImageJ software (right panel). Three blots were averaged (*t*-test, $*P < 0.01$). Bars indicate SD. In **(B)**, polyubiquitinated proteins ($(Ub)_n$) in insoluble fractions were immunologically detected. Three blots were quantitated as described in **(A)**.

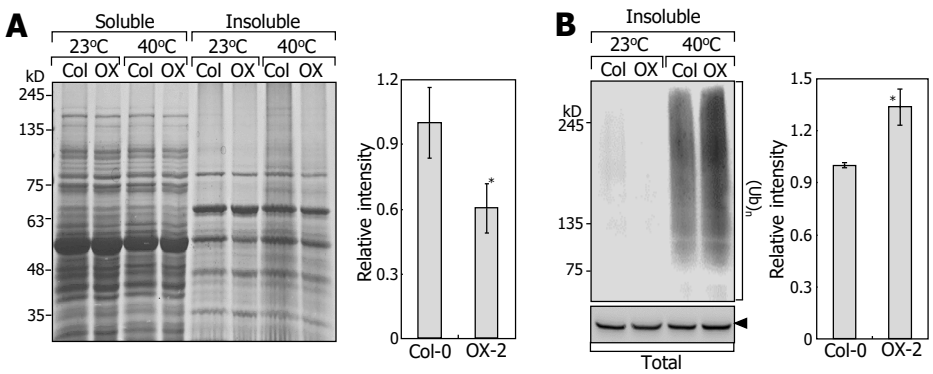

Figure 12. Levels of protein aggregates in ZTL-overexpressing OX-2 plants

Eight-day-old plants grown on MS-agar plates were transferred to MS liquid culture at 23°C for 1 d. At the midpoint of the day, they were then exposed to 40°C in darkness for 2 h before preparing soluble and insoluble fractions. In **(A)**, protein blots were stained with Coomassie blue (uppermost panel), and HSP90 and Tub were immunologically detected (lower panels). Relative levels of accumulated aggregates at high temperatures were quantitated using the ImageJ software (right panel). Three blots were averaged (*t*-test, $*P < 0.01$). Bars indicate SD. In **(B)**, polyubiquitinated proteins ($(Ub)_n$) in insoluble fractions were immunologically detected. Three blots were quantitated as described in **(A)**. Black arrowhead indicates Tub.

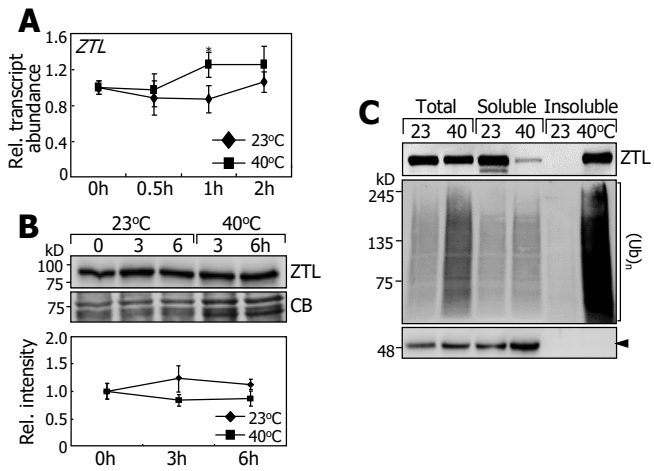

Figure 13. Effects of high temperatures on *ZTL* transcript abundance and its protein stability.

(A) and **(B)** Ten-day-old plants grown on MS-agar plates were exposed to 40°C. Transcript levels were examined by RT-qPCR **(A)**. Biological triplicates were averaged (*t*-test, $*P < 0.01$). Bars indicate SEM. The $35S_{pro}$*:ZTL-MYC* transgenic plants were heat-treated as described in **(A)**. ZTL-MYC proteins were immunologically detected **(B)**. CB, Coomassie blue-stained membrane.

(C) The $35S_{pro}$*:ZTL-MYC* transgenic plants were grown on MS-agar plates for 8 d and then were transferred to MS liquid culture at 23°C for 1 d. At the midpoint of the day, they were then exposed to 40°C in darkness for 2 h before preparing soluble and insoluble fractions. Protein fractions were prepared for the immunological detection of ZTL and $(Ub)_n$. Black arrowhead indicates Tub.

To verify the role of ZTL in clearing insoluble aggregates at high temperatures, I employed nano high-resolution LC-MS/MS spectrometry. Heat-induced insoluble protein bands were analyzed (Figure 14A), and several proteins that were predominant in the *ztl-105* mutant were identified (Figure 14B). I selected HEXOKINASE 1 (HXK1) as a representative protein for kinetic accumulation assays of insoluble aggregates. As expected, the level of HXK1 was significantly elevated in the *ztl-105* insoluble fraction at high temperatures (Figure 14C), showing that ZTL plays a role in clearing heat-induced protein aggregates.

ZTL interacts with HSP90 under normal conditions (Kim et al., 2011). The protein level of HSP90 increases after exposure to heat stress (Meiri and Breiman, 2009). I observed that both ZTL and HSP90 proteins are enriched in insoluble aggregates at high temperatures. I therefore examined whether the ZTL-HSP90 interaction is affected under heat stress. Bimolecular fluorescence complementation (BiFC) assays, which transiently express truncated yellow fluorescence protein fusions in *Arabidopsis* protoplasts, revealed that the ZTL-HSP90 interaction still occurred at high temperatures (Figure 15A). Notably, coimmunoprecipitation assays showed that the ZTL-HSP90 interaction was significantly elevated after heat shock (Figure 15B), indicating that high temperatures increase the formation of ZTL-HSP90 protein complexes.

The linkage of HSP90 with ZTL in heat-induced polyubiquitination was

further investigated using HSP90 RNAi plants, in which cytosolic HSP90 proteins are markedly depleted (Kim et al., 2011). Heat-induced polyubiquitination was markedly reduced in the HSP90 RNAi plants (Figure 15C), further supporting the functional linkage between ZTL and HSP90 in thermoinducible protein quality control.

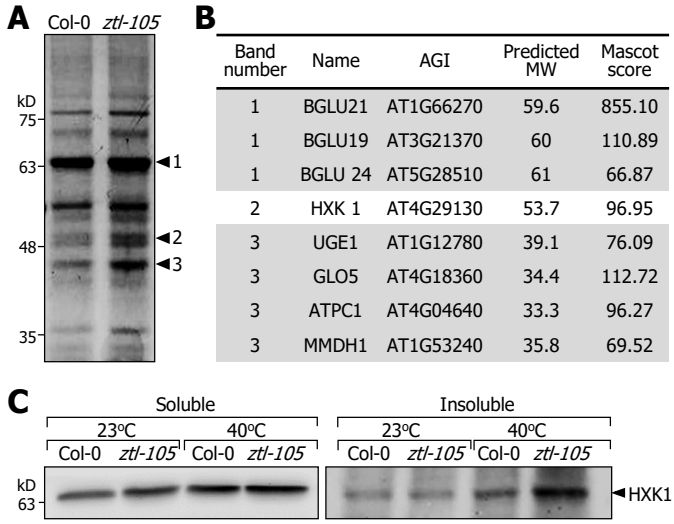

Band number	Name	AGI	Predicted MW	Mascot score
1	BGLU21	AT1G66270	59.6	855.10
1	BGLU19	AT3G21370	60	110.89
1	BGLU 24	AT5G28510	61	66.87
2	HXK 1	AT4G29130	53.7	96.95
3	UGE1	AT1G12780	39.1	76.09
3	GLO5	AT4G18360	34.4	112.72
3	ATPC1	AT4G04640	33.3	96.27
3	MMDH1	AT1G53240	35.8	69.52

Figure 14. Nano high resolution LC-MS/MS spectrometer analysis of protein aggregates at high temperatures.

(A) Levels of protein aggregates at high temperatures. Protein gels were stained with Coomassie blue.

(B) List of proteins identified by nano LC-MS/MS. Proteins were extracted from selected protein bands (as labeled 1 – 3 in **(A)**). The extracted proteins were subjected to nano high resolution LC-MS/MS. Some of the proteins that were predominant in the protein aggregates of *ztl-105* samples, including HXK1, are listed.

(C) Elevation of HXK1 protein levels in the insoluble aggregates from *ztl-105* mutant. Soluble and insoluble protein fractions were prepared from the heat-treated plants, as described above. Levels of HXK1 proteins were examined immunologically using an anti-HXK1 antibody.

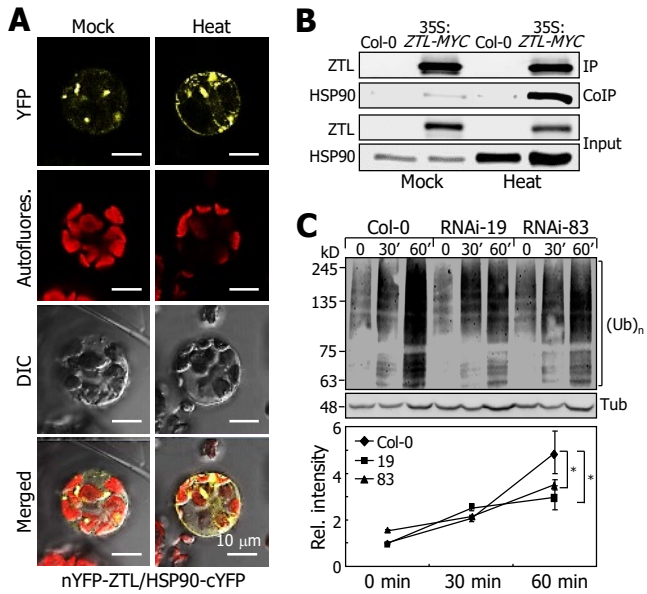

Figure 15. HSP90 is associated with heat-induced polyubiquitination by interacting with ZTL.

(A) BiFC on ZTL-HSP90 interaction. YFP, yellow fluorescent protein.

(B) Coimmunoprecipitation. The *35S$_{pro}$:ZTL-MYC* transgenic plants were exposed to 40°C in darkness for 2 h. Immunoprecipitation (IP) was performed using magnetic beads, and the precipitants were used for the immunological detection of MYC-ZTL and HSP90. Input represents 5% of the IP reaction.

(C) Reduction of heat-induced polyubiquitination in HSP90 RNAi plants. Plants were grown and exposed to 40°C. Polyubiquitinated proteins were detected immunologically. Three blots were quantitated and averaged (*t*-test, $*P < 0.01$). Bars indicate SEM.

The clock function is hypersensitive to high temperatures in the *ztl-105* mutant

My data indicate that ZTL is involved a protein quality control system functioning at high temperatures. It has been suggested that ZTL is involved in the temperature compensation of the circadian clock at warm temperatures (27ºC) (Edwards et al., 2005), raising the possibility that the ZTL-mediated thermal response is functionally associated with clock function.

I investigated circadian rhythms in the *ztl-105* mutant after exposure to high temperatures. At 28ºC, the rhythmic expression patterns of the gene encoding chlorophyll A/B-binding protein 2 (CAB2) remained unaffected but had reduced amplitudes in both Col-0 plants and the *ztl-105* mutant (Figure 16A). However, at 35ºC, both the phases and amplitudes of circadian rhythms were completely disturbed in the mutant, while circadian rhythms were still persistent but with a lengthened period in Col-0 plants (Figure 16B). These observations indicate that ZTL is required for robust clock function under heat stress but is not related to temperature compensation of the clock.

I found that HSP90 interacts with ZTL in modulating protein polyubiquitination at high temperatures (Figures 15). Circadian rhythms were disturbed in *ztl-105* mutant under identical conditions (Figure 16B). It was therefore suspected that circadian rhythms would be altered in plants having reduced HSP90 activity. Consistent with the known roles of cytosolic HSP90

proteins in clock function (Kim et al., 2011), circadian rhythms were largely disturbed in the HSP90 RNAi plants at high temperatures (Figure 17), as observed in the *ztl-105* mutant.

I next tested the linkage between accumulation of protein aggregates and clock thermosensitivity by including MG132, a potent proteasome inhibitor (Lee and Goldberg, 1998), in the assays on the circadian rhythmic expression of *CAB2* gene. At 23ºC, the rhythmic expression of *CAB2* gene was evident in both Col-0 plants and *ztl-105* mutant in the presence of MG132 (Figure 18). At 35ºC, the circadian rhythms were still evident at ZT24-48 but disappeared in the presence of MG132 (Figure 18A). In contrast, the rhythmic expression was not observed in *ztl-105* mutant even in the absence of MG132 (Figure 18B), demonstrating that ZTL plays a role in the thermostability of the clock by modulating the accumulation of protein aggregates.

It is known that ZTL modulates the protein stability of TOC1 and PRR5 through the ubiquitin-mediated degradation pathways (Más et al., 2003; Kiba et al., 2007). I therefore investigated whether ZTL-mediated control of TOC1 and PRR5 protein stability is related to the disrupted circadian rhythms in the *ztl-105* mutant at high temperatures. While the protein levels of TOC1 and PRR5 were rapidly reduced during the dark period at 23ºC (Figure 19A), such reductions were not observed at 35ºC (Figure 19B), similar to the protein accumulation patterns in

ZTL-defective mutants (Más et al., 2003; Kiba et al., 2007). In addition, TOC1 and PRR5 proteins remained in the soluble fraction (Figure 19C), while ZTL proteins were fractionated into the insoluble fraction (Figure 13C). These observations indicate that TOC1 and PRR5 are not directly involved in ZTL-mediated stabilization of the clock function at high temperatures.

Altogether, I report that the ZTL/HSP90-mediated protein quality control system confers sustainability of plant growth and, possibly, robust clock function under heat stress conditions. Upon exposure to stressful high temperatures, ZTL enhances the polyubiquitination of misfolded proteins to direct them toward the ubiquitin-proteasome pathways, thus eliminating the accumulation of protein aggregates that are toxic to cellular components. My data provides a distinct molecular link between protein quality control and thermotolerance response in plants.

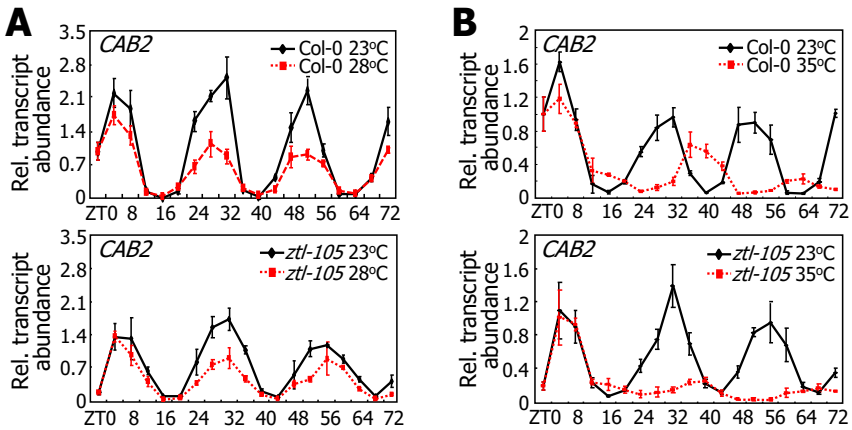

Figure 16. Disruption of circadian rhythms in *ztl-105* mutant at high temperatures.

Seven-day-old plants grown on MS-agar plates at 23°C were incubated at 28°C **(A)** or 35°C **(B)** in the light. Transcript levels were examined by RT-qPCR. Biological triplicates were averaged. Bars indicate SEM. ZT, zeitgeber time.

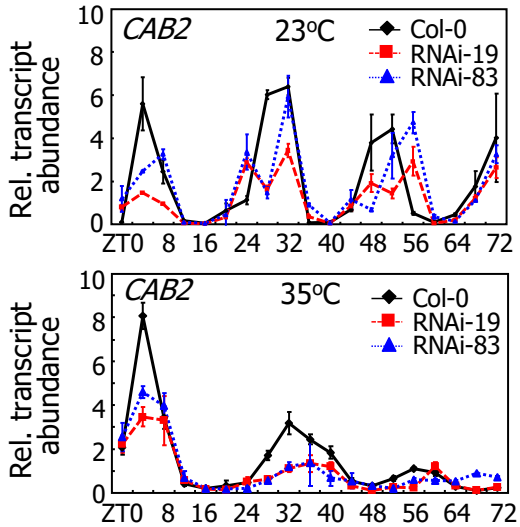

Figure 17. Disruption of circadian rhythms in HSP90 RNAi plants.

Seven-day-old plants grown on MS-agar plates at 23°C were incubated at 35°C in the light. Transcript levels were examined by RT-qPCR. Biological triplicates were averaged. Bars indicate SEM.

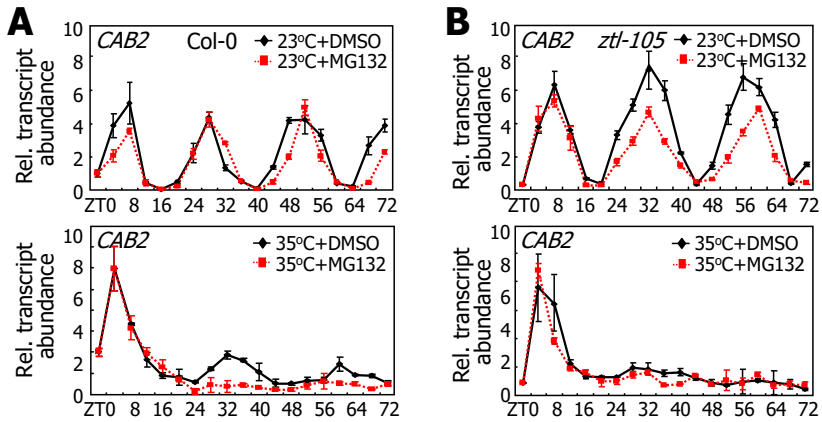

Figure 18. Effects of MG132 on circadian rhythms.

Six-day-old plants grown on MS-agar plates at 23°C were transferred to MS liquid culture for 1 d. They were then transferred to MS liquid culture supplemented with 50 μM MG132 and incubated at either 23°C or 35°C in the light. Circadian rhythms were examined in Col-0 plants **(A)** and *ztl-105* mutant **(B)**.

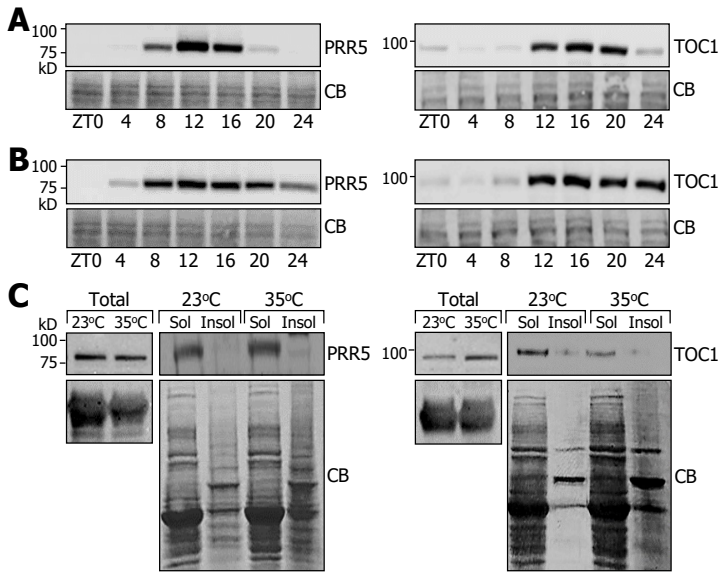

Figure 19. Diurnal rhythmic accumulation of PRR5 and TOC1 is disrupted at high temperatures.

(A) and **(B)** Accumulation patterns of PRR5 and TOC1 proteins. Plants were grown on MS-agar plates at 23°C for 9 d and then either kept at 23°C or transferred to 35°C for 1 d (**A** and **B**, respectively). PRR5-GFP and TOC1-YFP proteins were immunologically detected using polyclonal anti-GFP antibody produced in rabbit (catalog no. ab6556; Abcam). CB, Coomassie blue-stained membrane.

(C) Subcellular distribution of PRR5 and TOC1 proteins. The heat-treated transgenic plants described in **(A)** were used for the preparation of soluble and insoluble fractions. Parts of CB were displayed at the bottom for loading control.

DISCUSSION

ZTL and HSP90 mediate a thermoresponsive protein quality control mechanism

Protein misfolding is a common cellular event that occurs continuously as living organisms age or encounter environmental extremes, such as high temperatures and oxidative stress. Versatile protein quality control systems have evolved to cope with misfolded proteins and their insoluble aggregates by either facilitating refolding reactions or clearing insoluble aggregates (McClellan et al., 2005; Finka and Goloubinoff, 2013).

In plants, distinct ubiquitin-proteasome systems are responsible for the degradation of irreversibly aggregated proteins and the accompanying E3 ubiquitin ligase enzymes have been functionally characterized. The CHIP ubiquitin ligase polyubiquitinates misfolded proteins that are targeted for degradation to eliminate proteotoxicity under environmental stress conditions (Zhou et al., 2014; Lee et al., 2009; Samant et al., 2014). Meanwhile, the autophagy receptor neighbor of BRCA1 gene 1 (NBR1) mediates the autophagosomal degradation of ubiquitinated protein aggregates (Zhou et al., 2013). It has been shown that CHIP and NBR1 mediate two distinct but mutually complementary anti-proteotoxic pathways

working to respond to abiotic stresses in plants (Zhou et al., 2014).

Molecular chaperones are a group of proteins that not only facilitates proper folding of newly synthesized polypeptides but also mediates controlled degradation of misfolded proteins and their aggregates by forming chaperone-E3 ubiquitin ligase complexes (McClellan et al., 2005). Many molecular chaperones identified so far are HSPs, which are produced in response to elevated temperatures in plants (Zhou et al., 2014; Krishna and Gloor, 2001; Bita and Gerats, 2013). Among plant HSPs, HSP90 has been the most extensively studied in plant responses to environmental stresses, including defense mechanisms (Xu et al., 2012), phenotypic plasticity (Sangster and Queitsch, 2005), and buffering of genetic variations (Sangster et al., 2008). In particular, it has been found that high temperatures trigger HSP90 production, which plays a role in the assembly and maintenance of the 26S proteasome (Imai et al., 2003), suggesting a versatile role of HSP90 in shaping protein turn-over under stressful environments.

HSP90 plays a central role in maintaining animal circadian systems (Schneider et al., 2014). In plants, a well-known substrate of HSP90 is the F-box-containing ZTL ubiquitin ligase functioning in the circadian clock (Kim et al., 2011). It has been shown that HSP90 stabilizes ZTL and the HSP90-mediated maturation of ZTL is essential for clock function. The HSP90-mediated stabilization of ZTL also contributes to the rhythmic accumulation of tetrapyrroles

in chloroplasts, which in turn regulates the oscillated expression of genes encoding C-REPEAT BINDING FACTOR transcription factors (Noren et al., 2016). These observations support a potential role of the ZTL-HSP90 module in the intersection between the circadian clock and plastid signaling pathways.

In this study, I demonstrated that ZTL and HSP90 constitute a part of the proteasome-dependent protein quality control mechanism, which enhances the thermotolerance of plant growth and maintains thermostability of the clock function. In the ZTL-defective *ztl-105* mutant, protein polyubiquitination was reduced but insoluble protein aggregates accumulated. I also found that ZTL and HSP90 were cofractionated with insoluble aggregates under heat stress, indicating that the ZTL-HSP90-mediated protein quality control system plays a major role in the degradation of irreversibly misfolded proteins accumulating under heat stress. While the ZTL-HSP90 pathway thermostabilizes the clock function, it is not related with the temperature compensation of the clock.

The CHIP-defective mutants are thermo-susceptible, and insoluble protein aggregates accumulate in those mutants (Samant et al., 2014). Notably, polyubiquitination is elevated in the mutants, which is in contrast to the reduction of polyubiquitination in the *ztl-105* mutant and yeast mutants lacking various ubiquitin ligase enzymes (Fang et al., 2011; Yoo et al., 2015). This distinction suggests that the CHIP-mediated quality control mechanism is somewhat distinct

from those mediated by other E3 enzymes to maintain protein homeostasis.

ZTL sustains the thermostability of the circadian clock

It is currently unclear how the ZTL/HSP90 system confers enhanced high temperature tolerance to the clock function. One possibility would be that clock components or those mediating clock input and output signals are misfolded upon exposure to high temperatures, forming insoluble aggregates that disrupt protein homeostasis of the clock function. Under this circumstance, ZTL provides a finely tuned protein turnover mechanism targeting heat-induced aggregates of the clock components. Alternatively, the accumulation of denatured or damaged cellular proteins provokes cytotoxicity, resulting in overall dysfunction of cellular activities, including the clock function. I found that thermotolerance is reduced and circadian rhythms are disturbed in the *ztl-105* mutant at high temperatures, supporting the latter possibility.

Previous and my own data support that ZTL modulates the clock function under both normal and stressful conditions. It has been reported that the ZTL enzyme degrades TOC1 and PRR5 in a circadian rhythmic pattern (Más et al., 2003; Kiba et al., 2007). I found that HSP90 and ZTL accumulate in insoluble protein aggregates under heat stress. One plausible explanation is that ZTL plays dual roles in maintaining the clock function. Under normal temperature conditions,

it directs the dark-dependent degradation of TOC1 and PRR5 via the ubiquitin-proteasome pathway (Más et al., 2003; Kiba et al., 2007). On the other hand, when plants are exposed to high temperatures, ZTL and HSPs constitute a part of the proteasomal protein quality control machinery that eliminates insoluble protein aggregates inevitably occurring under this stressful condition. TOC1 and PRR5 remained soluble at high temperatures and were not targeted by the ZTL-HSP90 module, suggesting that ZTL mediates clock thermostability by targeting cellular proteins other than TOC1 and PRR5. The ZTL-mediated protein quality control system may also function under other stresses, such as oxidative stress and high salinity, which profoundly influence clock function (Marcolino-Gomes et al., 2014; Tamaru et al., 2013).

More work is required to elucidate the molecular mechanism that underlies the functions of ZTL and HSP90 in the heat-responsive protein quality control system. On the basis of their roles in plant thermotolerance and clock thermostability, the ZTL-HSP90 pathway would require additional cochaperones, such as HSP70 or GI. It is known that GI forms a ternary complex with HSP90 and ZTL, which functions in the maturation process of ZTL, to maintain the clock function under normal temperature conditions (Cha et al., 2017). It is likely that GI would also contribute to the thermotolerance response and clock thermostability by facilitating ZTL folding.

ACKNOWLEDGMENTS

I thank Dr. David Somers for providing the HSP90 RNAi lines. Woe-Yeon Kim analyzed the data and provided scientific discussion. Hyo-Jun Lee performed protein works.

CHAPTER 2

Auxin mediates the wind-induced development of adventitious roots in *Brachypodium distachyon*

INTRODUCTION

Plants are constantly challenged with surrounding environments and objects throughout their life cycles, among which the effects of different light regimes and temperatures have been extensively explored in terms of how plants sense these environmental signals and molecular mechanisms by which plants adapt to stressful environmental challenges. The reprogramming processes of plant growth and morphogenesis by light and thermal cues are termed photomorphogenesis and thermomorphogenesis, respectively (Arsovski et al., 2012; Quint et al., 2016).

Meanwhile, it has long been perceived by agricultural breeders and plant scientists that mechanical stimuli, including physical touch by passing animals, insect attack, raindrops, wind, and flooding, profoundly affect plant growth and morphogenesis. While plants growing indoors appear slender and spindly, those growing in wild habitats exhibit relatively short, thick stems but grow healthy and robust (Jaffe and Forbes, 1993). The mechanically induced reshaping of growth and morphology are often referred to as thigmomorphogenesis (Chehab et al., 2009). The thigmo-sensing process is considered to be an adaptation strategy that allows plants to cope with mechanical disturbances and thus is important for agricultural practices (Shah et al., 2017). It has been explored that plant growth hormones, such as auxin and ethylene (ET), mediate the thigmomorphogenic responses (Takahashi et al., 1984; Sarquis et al., 1991; Chehab et al., 2009), although detailed molecular mechanisms are largely unknown.

One of the most noticeable thigmomorphogenic responses is observed

with trees growing on the top area of mountains, where high wind speeds are common throughout the year. The mountain trees mostly appear stunted with relatively thick trunk and fewer branches because of a reduction in longitudinal stem growth that is accompanied by secondary radial stem growth (Biddington, 1986). Similar reshaping patterns of growth and morphology are also observed in Arabidopsis plants that are regularly exposed to wind gust (Braam and Davis, 1990). In extreme cases, wind-driven mechanical stress causes root and stem lodging and disorientation of the leaves, leading to a significant yield loss of cereal crops (Mi et al., 2011). In nature, windstorms impose severe hazarding effects on forests, such as tree damages and timber losses (Mitchell, 2013). Therefore, plants have evolved versatile adaptive strategies to cope with mechanical wind forces. The wind-responsive morphological changes allow plants to avoid stem breakage and uprooting by building a rigid architecture and minimizing the force from wind (Gardiner et al., 2016).

The phenomenon of plant acclimation to wind stress has been documented for decades in different plant species. However, the modes of plant responses to wind-induced mechanical stimulation vary greatly among different plant species, depending on the intensity and timing of the stimuli (Urban et al., 1994; Gillies et al., 2002; Badel et al., 2015), and thus how plants sense and transmit the wind-derived signals to appropriate physiological responses is largely unknown in most cases. Especially, wind-driven thigmomorphogenic responses also include the rearrangement of biomass to the root systems and the restructuring of the root growth and patterning (Coutand et al., 2008).

While it is increasingly evident that the aboveground wind affects the root growth and architecture, the thigmomorphogenic responses of the root system have not been explored extensively because it is influenced by a complicated network of both the aboveground and soil conditions. For example, it has been observed that soil conditions, such as soil particle composition, nutrient contents and composition, and water content influence the root responses to wind (Reubens et al., 2009).

Recent studies have provided an invaluable hint for elucidating molecular mechanisms governing root thigmomorphogenesis. Adventitious roots (ARs) are formed from nonroot tissues naturally in numerous plant species under both normal and stressful growth conditions (Steffens and Rasmussen, 2016). In cereal crops, including wheat, rice, and maize, the ARs are important for plant adaptation to various stress conditions, such as flooding, drought, soil burial, and nutrient deficiency. However, it is still unclear how plants sense surrounding signals to launch downstream molecular events in triggering AR formation.

One of the best described is the AR formation in rice (Oryza sativa). In this plant species, AR development is initiated both during normal development and in response to stressful stimuli (Steffens and Sauter, 2009). It is known that the AR formation is mediated by LATERAL ORGAN BOUDARIES DOMAIN (LBD), ADVENTITIOUS ROOTLESS1 (ARL1), and WUSCHE RELATED HOMEOBOX11 (WOX11) transcription factors (Liu et al., 2005; Zhao et al., 2009). Accordingly, ARL1-deficient rice mutants do not form ARs (Liu et al., 2005). The *ARL1* gene is responsive to auxin and ethylene signals and mainly expressed in lateral and AR primordia, tiller primordia, and vascular tissues (Liu et

al., 2005). ARL1 is known to act as a regulator of auxin-mediated cell dedifferentiation and promotion of cell division (Liu et al., 2005). Meanwhile, WOX11 plays a role in cytokinin and auxin signaling networks during AR development (Zhao et al., 2009). It is involved in both AR emergence and growth, coordinating auxin and cytokinin signaling cascades that stimulate cell division (Zhao et al., 2009). However, it has been unexplored whether the auxin-mediated AR formation is associated with wind-induced thigmomorphogenic root growth.

In this study, I systematically investigated how *Brachypodium distachyon*, a widely used monocot model in recent years, adapts to wind-mediated mechanical stress. It was found that in response to constant wind gust, Brachypodium develops shoot-born ARs from the leaf nodes, which strengthen the statue of the plant against stem and root lodging. Interestingly, direct contact of the leaf nodes with soil particles, not the bending of the mesocotyls, is the major stimulating cue that induces AR formation through WOX- and LBD-mediated auxin signaling pathways. My findings demonstrate that the wind-induced stimulation of thigmomorphogenic AR formation is essential for the enhancement of mechanical tolerance and rapid recovery from stem flattening in Brachypodium and perhaps related grass species as well.

MATERIALS AND METHODS

Plant materials and growth conditions

Brachypodium distachyon ecotype Bd21-3, a standard diploid inbred line widely used in the community, was used in all assays. The seeds without lemma were placed on two layers of wet filter paper at 4 ºC for seven days. The germinating seedlings were then transferred to soil and grown in a controlled growth chamber with relative humidity of 60% under long day conditions (16-h light and 8-h dark). Growth temperatures were set at 23 ºC with white light illumination with a light intensity of 150 μmol photons/m^2s provided by FLR40D/A fluorescent tubes (Osram, Seoul, Korea).

Phenotypic analysis

For wind treatments, an electronic fan (EF-73HK, Hanil, Korea) was used and, and the speed of wind flow was measured by anemometer (ST-112, Sincon, Korea). For wind acclimation analysis, three-week-old plants grown in soil were first exposed to a constant unidirectional wind flow (1.9 m/s) for ten days. Following the pretreatment, the wind-acclimated plants were subjected to wind flow and photographed. Wind sensitivity was analyzed by measuring the angles of fluttered leaves relative to the soil surface.

To examine the effects of AR dissection, three-week-old plants grown in soil were exposed to a constant unidirectional wind flow for ten days. The plants

harboring ARs were identified, and visible ARs were dissected. The AR-dissected or -retaining plants were subjected to wind flow, and leaf angles were measured.

For examine the effects of falling down of the leaf nodes, three-week-old plants grown in soil were artificially fallen down using arresting wire so that the leaf nodes directly touch the soil particles. Arresting wires were carefully equipped not to touch the leaf node parts because they would potentially trigger a touch-induced thigmomorphogenic response. Ten days following the falling down setup, the frequency of AR emergence was measured, in which ARs longer than 5 mm in length were counted. For gravi-stimulation assays, plants were rotated by 75 degrees and further grown for ten days. To maintain the horizontally positioned stems and leaf nodes, plants were equipped with supporting wires. For assays on the effects of a combined stimulation of gravity and falling down, artificially fallen plants were rotated to position vertically the stems and leaf nodes. One side of the leaf nodes was allowed to be in direct contact with soil particles. The plants were further grown for ten days before assays.

To examine the potential effects of mechanical touch on the induction of AR emergence, the leaf nodes of three-week-old plants was completely covered with soil or sand stack. In addition, two layers of miracloth were laid in between the sand stack and the grounding soil layer to keep the sand stack in a semidry state.

Chemical treatments

The auxin transport inhibitor NPA (Sigma, St. Louis, MO, USA) and the ET perception inhibitor $AgNO_3$ (Sigma) solutions were prepared in Tween 20

(Amresco, Radnor, PA, USA). NPA (1 μM in 0.05% (v/v) aqueous Tween 20) or $AgNO_3$ (1 μM or 100 μM in 0.5% (v/v) aqueous Tween 20) was sprayed once a day for ten days onto three-week-old plants grown in soil, each spray using approximately 1 ml per plant. After the first spray, plants were artificially fallen down and further grown for ten days before analysis.

For gene expression assays, NPA (1 mM in 0.05% (v/v) aqueous Tween 20) or IAA (Sigma, 100 μM in 0.5% (v/v) aqueous Tween 20) were sprayed onto three-week-old plants, which were subsequently fallen down. The leaf nodes and their internodes were harvested at 0, 3, 6, 12, and 24 h following chemical treatments into liquid nitrogen for the extraction of total RNA samples.

Phylogenetic analysis

The amino acid sequences of the WOX proteins from Brachypodium (*BdWOX6*, *BdWOX7*, *BdWOX10*, *BdWOX11*, and *BdWOX12-like*), Arabidopsis (*AtWOX11*, and *AtWOX12*), and rice (*OsWOX11*) were obtained from NCBI (https://www.ncbi.nlm.nih.gov/pubmed). The amino acid sequences of the LBD proteins from Brachypodium (*BdLBD1*, *BdLBD4*, *BdLBD6*, *BdLBD15*, *BdLBD20*, *BdLBD30*, and *BdLBD36*) and rice (*OsARL1*) were similarly obtained from NCBI. Phylogenetic analysis was carried out using the MEGA 7 software (https://www.megasoftware.net/).

Gene transcript analysis

Total RNA was extracted from appropriate plant materials using the RNeasy Plant

Mini Kit (Qiagen, Valencia, CA) according to the manufacturer's procedure and thoroughly pretreated with a RNase-free DNase to get rid of contaminating genomic DNA before use. Reverse transcription-mediated real-time PCR (RT-qPCR) was employed to analyze the levels of transcripts.

All RT-qPCR reactions was performed in 96-well blocks with the Applied Biosystems 7500 Real-Time PCR System (Foster City, CA) using the SYBR Green I master mix in a reaction volume of 20 μl. The two-step thermal cycling profile employed was 15 s at 95°C for denaturation and 1 min at 60-65°C, dependi ng on the calculated melting temperatures of PCR primers, for annealing an d polymerization. An *UBC18* gene (Bd4g00660) was included as internal co ntrol in the PCR reactions to normalize the variations in the amounts of pri mary cDNAs used. The PCR primers were designed using the Primer Express software installed in the system and listed in Table S2.

Statistical analysis

All experiments were conducted using biologically independent samples, and the number of biological replicates is given for each experiment. Statistical significance was determined using either one-way analysis of variance (ANOVA) with *post hoc* Tukey test or Student *t*-test for determining significant differences or pairwise comparisons, respectively.

Primers			Usage	Sequence
UBC18	(Bradi4g00660)	F	RT-qPCR	5′-GGAGGCACCTCAGGTCATTT
		R	RT-qPCR	5′-ATAGCGGTCATTGTCTTGCG
WOX10	(Bradi3g18800)	F	RT-qPCR	5′-CACGGCATCATGCACTACGG
		R	RT-qPCR	5′-AGGTTTCTGTGTACCGGTGG
WOX11	(Bradi1g18420)	F	RT-qPCR	5′-CTGCTGCTCTCTCGCAATCG
		R	RT-qPCR	5′-AAGACGACCCGGACCCATA
LBD20	(Bradi1g75110)	F	RT-qPCR	5'-AGCTCGCATCCTTCAAGCAG
		R	RT-qPCR	5'-ATTGTTGCCACCGTAAACGC
LBD30	(Bradi1g68170)	F	RT-qPCR	5'-CAGGTGGTGAATCTCCAGGC
		R	RT-qPCR	5'-AAGAGTGCGGAGAGGTCGAT
UGT76-4	(Bradi4g41410)	F	RT-qPCR	5'-ATTCTCCTCTCCGCAACAGA
		R	RT-qPCR	5'-CGGTTAAGCTCCTGCTCTTG
TAR2	(Bradi2g04290)	F	RT-qPCR	5'-GGCTCCATACTACTCTTCGTATC
		R	RT-qPCR	5'-CAGTAGTAGGCCAGGTCGTG
MT2b	(Bradi2g62315)	F	RT-qPCR	5'-CGGAGGAAACTGCAACTGCG
		R	RT-qPCR	5'-GAGGAGGCTGGAGGTCTGGA

Table 2. Primers used in CHAPTER 2.

The primers were designed using the Primer3 software in a way that they have calculated melting temperatures in a range of 50 - 65 ºC. F and R indicate forward primer and reverse primer, respectively.

RESULTS

Brachypodium adapts to wind-induced mechanical stress by forming ARs

Several tree species and cereal crops have been shown to adapt to stressful mechanical stimuli by altering their growth and morphology (Biddington, 1986; Reubens et al., 2009). Wind is one of the critical climate factors in crop agriculture that greatly affect the annual yields of crops. Considering that Brachypodium shares many morphological and developmental traits with crop species (Brkljacic et al., 2011), I decided to elucidate how this plant species withstands wind stress at the molecular level.

I first conducted a series of wind exposure assays, in which wind-acclimated and nonacclimated plants were exposed to constant unidirectional wind flow for ten days. It was found that wind-acclimated plants exhibited a relatively reduced bending of mesocotyls (Figure 20A). Plant resistant responses to wind force were then quantified by measuring leaf angles relative to the horizontal plane. While the leaf angle was approximately 30 degrees in nonacclimated plants, it was larger than 60 degrees in wind-acclimated plants (Figure 20B), showing that Brachypodium is capable of adapting to wind-mediated mechanical force.

I next investigated growth and morphological changes that accompanied wind acclimation. Overall plant morphology and growth patterns in the aerial plant

parts were not discernibly affected by wind treatments in my assay conditions (Figure 20). Interestingly, I found that more ARs were formed from the leaf nodes of the tillers in wind-treated plants (Figure 21), raising a possibility that AR formation is responsible for the wind-tolerant phenotype. To examine this possibility, I dissected the ARs of the wind-treated plants and performed an additional round of wind treatments. While AR-intact plants exhibited wind tolerance, AR-dissected plants exhibited a significant reduction of wind tolerance (Figure 21B). These observations indicate that the wind-induced formation of ARs from the leaf nodes of the tillers is functionally associated with wind tolerance and the ARs help plants support the aboveground shoots against wind.

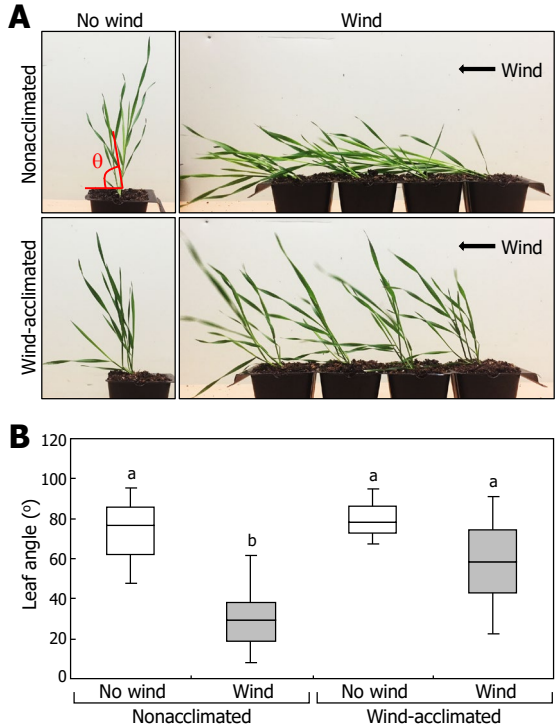

Figure 20. Adaptation of *Brachypodium* plants to wind-induced mechanical stimulation.

Three-week-old plants grown in soil were either exposed to a constant unidirectional wind flow or grown under control conditions for 10 days (wind-acclimated or nonacclimated, respectively) and subjected to wind treatments.

(A) Leaf fluttering phenotypes.

(B) Effects of wind flow on leaf angle. Wind-treated plants were photographed, and the largest leaf angles were measured. Box plots show the range of measured leaf angles ($n > 20$). Different letters represent a significant difference ($P < 0.01$) determined by the Tukey's honestly significant difference (HSD) test.

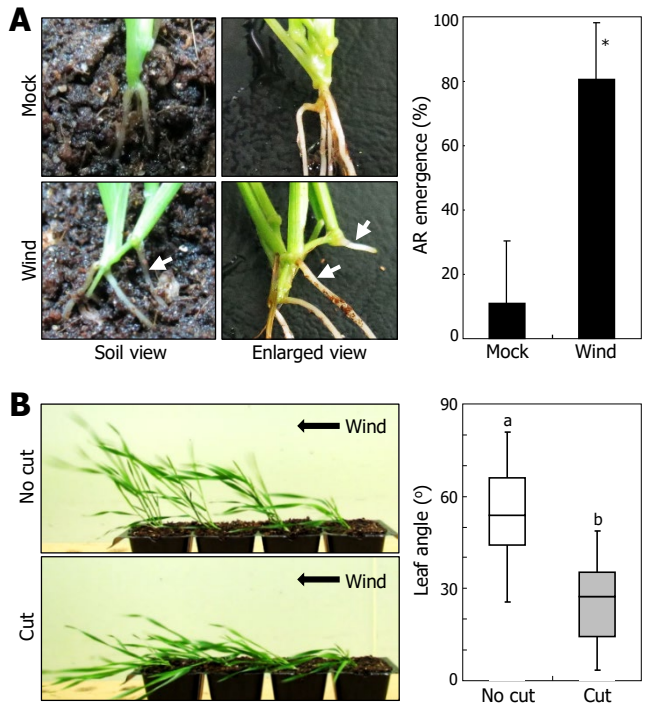

Figure 21. Induction of AR formation by wind stimulation.

Three-week-old plants were either grown under control conditions (mock) or exposed to a unidirectional wind flow (wind) for 10 days prior to analyzing AR formation.

(A) AR emergence. Leaf node roots formed on tillers were counted as ARs (right graph). ARs formed in the soil-grown plants and their enlarged views were displayed (left photographs). White arrows indicate ARs. Sixteen plants were measured in two independent experiments and statistically analyzed (Student *t*-test, $*P < 0.01$). Error bars indicate standard error of the mean (SEM).

(B) Wind responses of plants with or without ARs. Visible ARs of unidirectional

wind-treated plants were either retained (no cut) or dissected (cut), and the plants were exposed to wind stimulation (left photographs). Leaf angles were measured and statistically analyzed (right graph, $n = 20$). Different letters represent a significant difference ($P < 0.01$) determined by the Tukey's HSD test.

Wind-driven falling down of the shoots triggers AR formation

A visible effect of wind on plants is the mechanical falling down of the aerial plant parts. Wind also imposes changes in aerial pressure and plant body temperature. A critical question was whether the wind-driven falling down of the shoots is the major determinant of AR formation or additional physicochemical factors are required for the wind-tolerant process.

Prior to wind treatments, Brachypodium plants were equipped with supporting wire so that the shoots do not fall down even under windy conditions (Figure 22A). Notably, plants equipped with supporting wire, which do not fall down in response to wind, exhibited a significantly reduced emergence of ARs (Figure 23), suggesting that the wind-induced mechanical falling, not other effects of wind, such as changes in aerial pressure and temperature, is the major factor that triggers the induction of AR emergence under wind-mediated stress conditions.

Mechanical bending of the mesocotyls positions the leaf nodes horizontally, rotating the direction of gravity 90 degrees in these plant organs. Gravi-stimulation is known to induce lateral root emergence in Arabidopsis (Ottenschläger et al., 2003). I therefore examined whether the gravity affects the frequency of AR emergence. Plants grown in soil were either artificially fallen down using arresting wire or rotated horizontally and further grown for ten days (Figure 22B and Figure 22C, respectively). Artificially fallen plants exhibited a

frequency of AR emergence similar to what observed with wind-treated plants (Figure 24A). In contrast, gravi-stimulated plants exhibited a markedly reduced frequency of AR emergence compared to those in wild-treated and artificially fallen plants. A combined stimulation by gravity and falling down recovered the frequency of AR emergence comparable to that observed in wind-treated and artificially fallen plants (Figure 24B). It was notable that in plants stimulated by artificial falling down and gravity, ARs were formed mostly from the soil-contacting side of the leaf nodes (Figure 24B, white arrow). Together, these observations suggest that while direct soil contact of leaf node by mechanical bending of the mesocotyls is a major determinant of the AR formation, gravi-stimulation plays a minor role, if any, in the root thigmo-adaptation process.

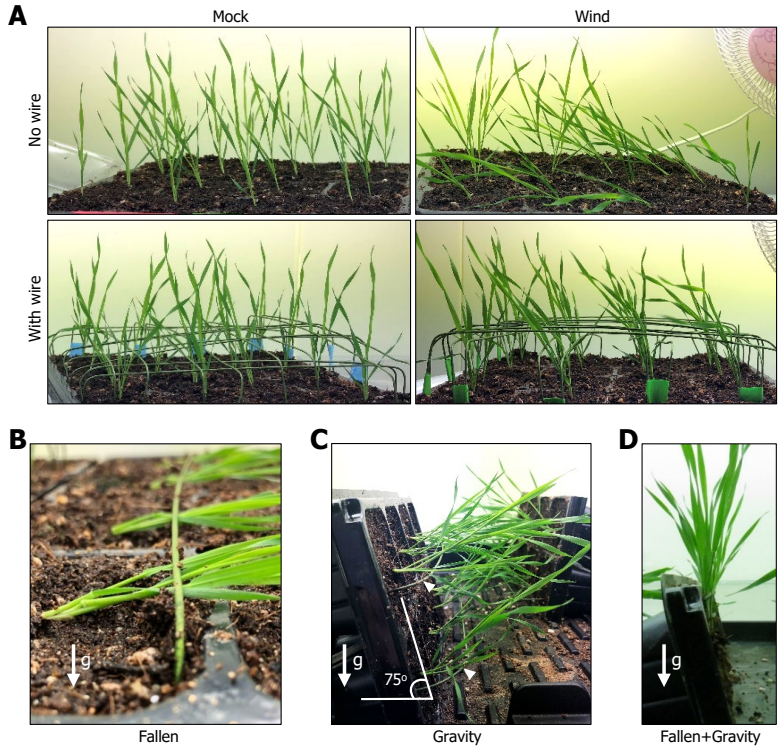

Figure 22. Experimental set-up for phenotypic analysis of plants against mechanical and gravity stimuli.

(A) Experimental set-up.

(B-D) Experimental set-up for 'falling' and 'gravity' stimuli. Plants were artificially fallen down to the soil surface by wire (**B**). Plants were gravistimulated by rotating horizontally (**C**). To prevent the shoots from falling downward, plants were supported by wire (arrowheads). The supporting wires were arranged carefully not to touch the leaf nodes. Artificially fallen plants were rotated by 75°, allowing them to grow upward (**D**). Note that only one side of the leaf nodes was soil-touched.

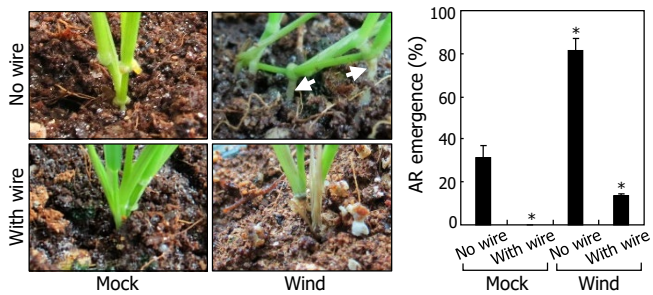

Figure 23. Effects of wind-driven falling down on AR formation.

Three-week-old plants grown in soil were further grown for 10 days under windy conditions with or without supporting wire. Following wind treatments, representative plants were photographed (left photographs). AR emergence was statistically analyzed (right graph). Sixteen plants were measured in three independent experiments and statistically analyzed using Student *t*-test (*$P < 0.01$). Error bars indicate SEM. White arrows indicate ARs.

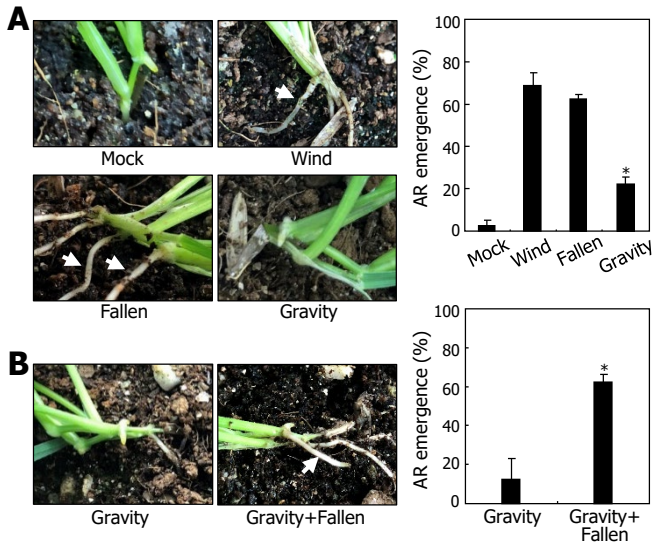

Figure 24 Effects of mechanical and gravity stimuli on AR formation.

Three-week-old plants grown in soil were further grown for 10 days under various conditions. Sixteen plants were measured in three independent experiments and statistically analyzed using Student *t*-test (*$P < 0.01$). Error bars indicate SEM. White arrows indicate ARs.

(A) Plants were artificially fallen down using wire (fallen). Plants were also grown on a slope of 75° to impose gravity stimulation (gravity). Following treatments, representative plants were photographed (left photographs). AR emergence was statistically analyzed (right graph).

(B) Effects of combined stimulation of gravity and falling down on AR formation. Plants were fallen down and then rotated by 75° to impose combined stimulation. Representative plants were photographed (left photographs), and AR emergence was statistically analyzed (right graph).

Direct contact of the fallen leaf nodes with soil particles triggers the induction of AR emergence

I found that ARs are formed in the soil-contacting side of fallen plants (Figure 24B). In addition, the bending of the mesocotyls and the horizontal positioning of the leaf nodes do not induce AR formation (Figure 24B). I therefore speculated that direct soil contact is a prerequisite for the induction of AR formation.

To test the hypothesis, plants were artificially fallen down, and the leaf node parts were embedded in the soil (soil-embedded). The occurrence of AR emergence was counted on the upper and lower sides of the soil-embedded lead nodes. Surprisingly, soil-embedded leaf nodes produced multiple ARs on both the lower and upper sides, unlike fallen plants that produced ARs mostly on the lower, soil-contacting side of the leaf nodes (Figure 25). It was therefore evident that direct contact with soil particle is critical for AR formation.

A next question was whether direct contact with soil particles routinely used for Brachypodium culture is sufficient for the induction of AR formation. Plants were covered with the soil up to the leaf nodes but without the bending of the mesocotyls. Notably, the soil-covered plants formed ARs around the leaf nodes (Figure 26), strongly supporting that mechanical contact with soil particles, not the bending of the mesocotyls, is sufficient for the induction of AR emergence.

It has been reported that soil nutrient conditions affect AR emergence and

its elongation at the leaf nodes in Brachypodium (Poiré et al., 2014). To eliminate or reduce the effects of nutrients in the covering soil layer, fine sand particles that were thoroughly rinsed with water were stacked to cover the second leaf nodes. Under this condition, the leaf nodes were assumed to be exposed mostly to mechanical contact, and the effects of soil nutrients, if any, were supposed to be negligible. The sand particle-covered plants still formed ARs around the leaf nodes at the frequency comparable to that observed in the soil-covered plants (Figure 26). In the meantime, water logging is a well-known factor that triggers AR formation in various plant species (Steffens et al., 2006; Vidoz et al., 2010). I put miracloth in between the sand stack and the soil layer to get rid of the majority of water from the sand stack. Under this experimental condition, the frequency of AR emergence was comparable to those observed in the plants covered with the soil layer or the sand stack alone. Together, these observations unequivocally demonstrate that mechanical contact with the solid particles, not soil nutrients nor water logging, provokes AR emergence in Brachypodium.

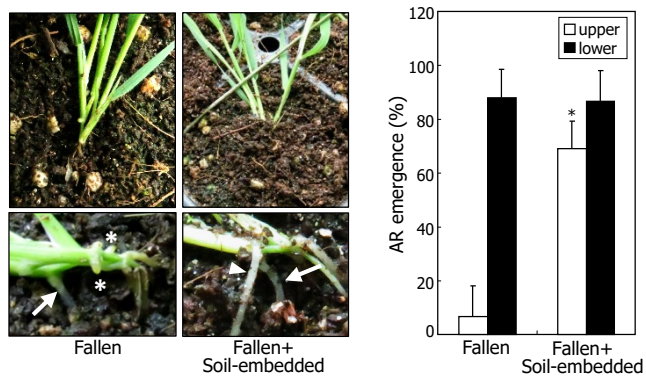

Figure 25. Induction of AR formation by soil contact.

Three-week-old plants grown in soil were further grown for 10 days under experimental conditions. White arrows indicate ARs. The leaf nodes of the fallen plants were then embedded in soil (fallen+soil-embedded) for 10 days. Representative plants were photographed (left photographs). Arrows and arrowheads indicate ARs formed at the lower and upper sides of the fallen tillers, respectively. Asterisks mark AR primordia. AR emergence was statistically analyzed (right graph). Sixteen plants were measured in three independent experiments and statistically analyzed using Student *t*-test (*$P < 0.01$). Error bars indicate SEM.

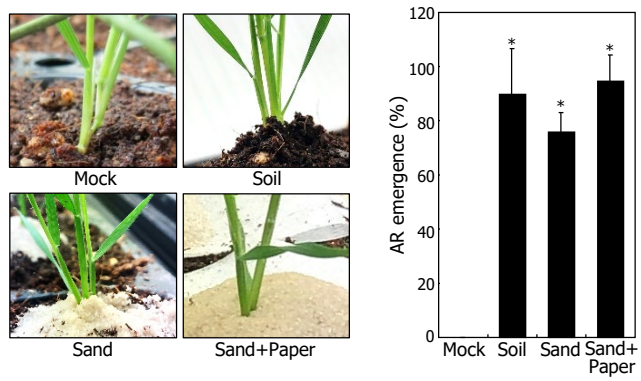

Figure 26. Induction of AR formation by sand-driven mechanical touch.

Leaf nodes were covered with soil or sand stack (left photographs). To maintain the sand stack in a minimally soaked state, miracloth was laid in between the sand and soil stacks (sand+paper). AR emergence was statistically analyzed (right graph). Sixteen plants were measured in three independent experiments and statistically analyzed using Student *t*-test (*$P < 0.01$). Error bars indicate SEM.

Auxin mediates the wind-mediated mechano-stimulation of AR emergence

Auxin is one of the key growth hormones that mediate root morphogenesis (Sabatini et al, 1999; Casimiro et al., 2001; Dubrovsky et al., 2008). ET is another growth hormone that is known to play a role in the induction of AR emergence under stressful conditions, as observed with submergent plants in flooded areas (Steffens et al., 2006; Vidoz et al., 2010). My observations indicate that ARs formed mostly at the leaf nodes that are directly contacted with soil particles.

To obtain insights into how mechanical stimulation by direct contact with soil particles mediates the induction of AR emergence, I employed chemicals that specifically inhibit auxin or ET functioning. The plant shoots were treated with either an auxin transport inhibitor, *N*-1-Naphthylphthalamic acid (NPA), or an ET perception inhibitor, $AgNO_3$ (Thomson et al., 1973; Beyer, 1976). The inhibitor-treated plants were then artificially fallen down using arresting wire so the leaf nodes were directly contacted with soil particles. It was found that application of NPA significantly reduced the frequency of AR emergence, while application of AgNO3 slightly increased the incidence of ARs (Figure27). Application of a higher concentration of $AgNO_3$ also showed a similar tendency, a slight increase of AR emergence (Figure 28). These observations suggest that auxin plays a major role in inducing the mechano-stimulation of AR formation in Brachypodium.

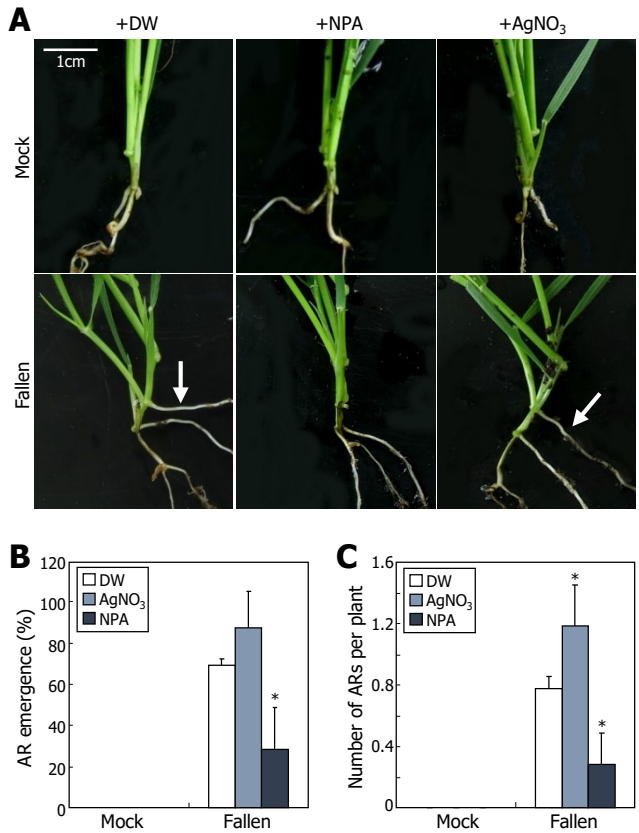

Figure 27. Auxin-mediated induction of AR formation in fallen plants.

(A-C) Effects of growth hormone inhibitors on AR formation. Three-week-old plants grown in soil were artificially fallen down, and a NPA or $AgNO_3$ solution (1 mM) was sprayed once a day for 10 days. Representative plants were photographed (**A**). Arrows indicate ARs. DW, double-distilled water. AR emergence (**B**) and number of ARs per plant (**C**) were measured. Sixteen plants were measured in three independent experiments and statistically analyzed (*t*-test, $*P < 0.01$). Error bars indicate SEM.

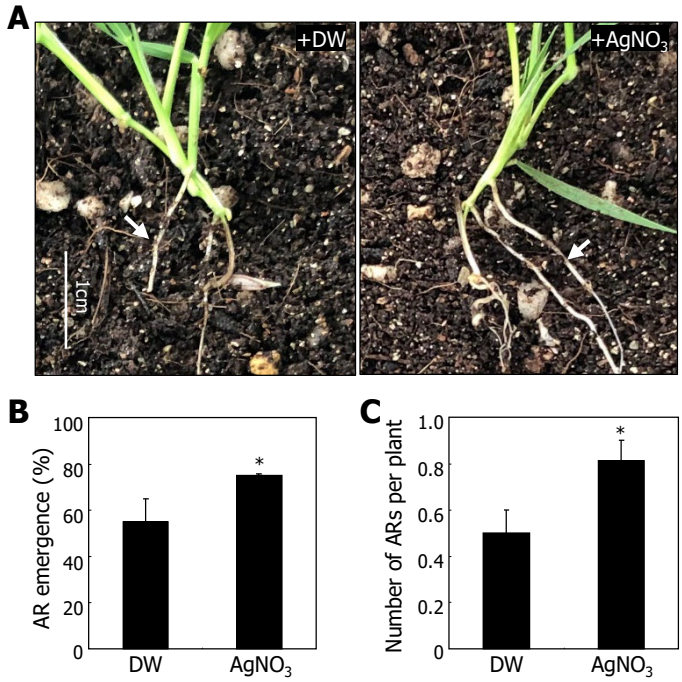

Figure 28. Effects of ethylene inhibitor on AR formation.

Three-week-old plants grown in soil were artificially fallen down, and a solution of 0.1 mM $AgNO_3$ was sprayed once a day for 10 days. Representative plants were photographed (**A**). White arrows indicate ARs. Sixteen plants were measured in two independent experiments and statistically analyzed (*t*-test, $*P < 0.01$) for AR emergence (**B**) and number of ARs per plant (**C**). Error bars indicate SEM.

WOX and *LBD* genes are auxin-responsive in artificially fallen plants

In Arabidopsis, while AR formation does not occur under normal growth and developmental conditions, molecular genetic studies have shown that the plant-specific WOX transcription factors, such as AtWOX11 and AtWOX12, function as key regulators of the induction of AR formation during organogenesis (Liu et al., 2014). Similarly, a rice homolog of the WOX members, OsWOX11, is attributed to the initiation and development of crown roots (Zhao et al., 2009).

Phylogenetic analysis revealed that there are a group of WOX proteins in the Brachypodium genome (Figure 29A). Amino acid sequence analysis revealed that among the Brachypodium WOX members, BdWOX10 and BdWOX11 shared a high sequence similarity with Arabidopsis AtWOX11 and AtWOX12. On the basis of the notion that auxin is a key regulator of the wind-induced AR formation in Brachypodium, I examined whether the *BdWOX10* and *BdWOX11* genes are responsive to auxin. Plants were sprayed with indole-3-acetic acid (IAA) or NPA and artificially fallen down. The leaf nodes, a major sites of AR formation in Brachypodium, and their internodes were then harvested for gene expression assays. It was found that the transcription of the *BdWOX10* and *BdWOX11* genes were induced by more than 10-fold by exogenous auxin application but drastically suppressed to a basal level by NPA (Figure 29B).

ADVENTITIOUS ROOTLESS1 (ARL1) is a rice homolog of the LBD

transcription factors (Liu et al., 2005). It has been shown that rice mutants lacking the ARL1 gene is not able to induce AR formation (Liu et al., 2005). Phylogenetic analysis revealed that BdLBD20 and BdLBD30 constitute a clade with the rice ARL1 (OsARL1) (Figure 30A). Gene expression assays showed that the transcription of the *BdLBD20* and *BdLBD30* genes was significantly induced by exogenous auxin application but suppressed by NPA (Figure 30B), similar to the effects of auxin and NPA on the *BdWOX* genes. These observations suggest that the BdWOX and BdLBD proteins are functionally associated with the wind-induced mechano-stimulation of AR formation in Brachypodium.

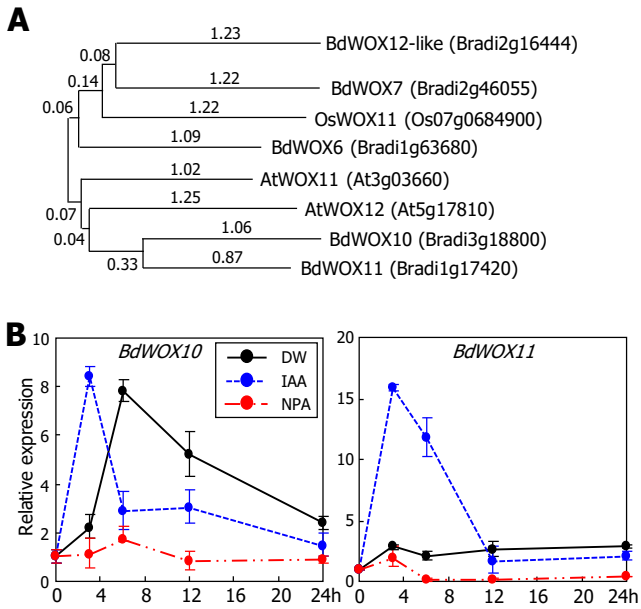

Figure 29. Auxin-mediated stimulation of *WOX* gene expression in falling-induced AR formation.

(A) Phylogenetic analysis of WOX proteins in *Brachypodium*. The phylogenetic tree was generated using the Neighbor-Joining method of the MEGA7 software (https://www.megasoftware.net).**B)** Effects of auxin and NPA on the transcription of *Brachypodium WOX* genes. Three-week-old plants grown in soil were sprayed with 0.1 mM IAA or 1 mM NPA solution and then artificially fallen down to the soil surface. The leaf nodes and their internodes were harvested at the indicated time points following mechanical stimulation. Transcript levels were analyzed by RT-qPCR. Biological triplicates, each consisting of 15 independent plants, were averaged. Error bars indicate SEM.

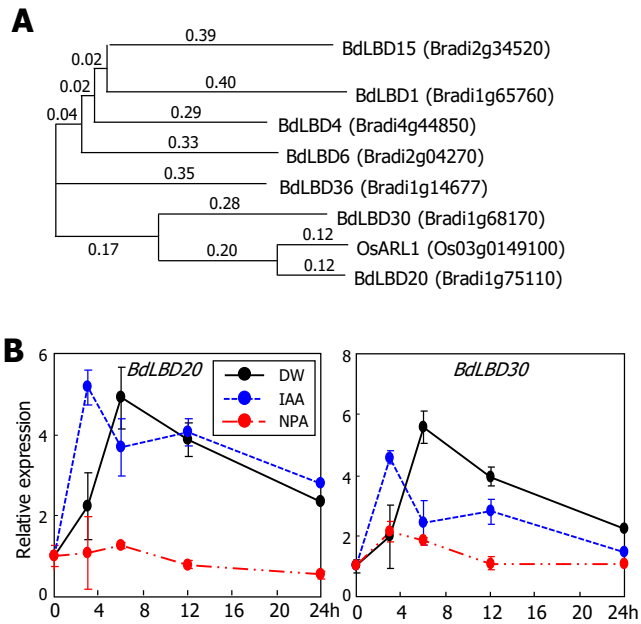

Figure 30. Auxin-mediated stimulation of *LBD* gene expression in falling-induced AR formation.

(A) Phylogenetic analysis of LBD proteins in *Brachypodium*. Note that BdLBD20 and BdLBD30 form a clade with OsARL1.

(B) Effects of auxin and NPA on the transcription of *LBD* genes. Plant growth and RT-qPCR were performed as described in Figure 29B.

***WOX* and *LBD* genes are induced by the wind-mediated mechano-stimulation**

A last question was whether the BdWOX and BdLBD proteins are functionally linked with the wind-induced mechano-stimulation of AR formation. I examined whether the expression of the auxin-responsive *BdWOX* and *BdLBD* genes is altered in response to mechanical stimuli. Gene expression assays showed that the auxin responsiveness of their transcriptions reaches the peak 6 hours following auxin treatments (Figures 29 and 30). Therefore, plant materials were harvested 6 hours following mechanical treatments. As inferred from the notion that the *BdWOX* and *BdLBD* genes are involved in lateral root development or AR formation in rice and Arabidopsis (Liu et al., 2005; Zhao et al., 2009; Liu et al., 2014), their transcriptions were markedly induced by wind treatments and falling down of the mesocotyls (Figure 31A and 31C), strongly supporting that the BdWOX and BdLBD transcription factors are involved in the wind-stimulated AR formation in Brachypodium.

Genes encoding UDP-glycosyltransferase 76C2-like (UGT76-4) and tryptophan aminotransferase-related protein 2-like (TAR2) are known as ethylene response markers in Brachypodium (Kouzai et al., 2016). Metallothionein2b (MT2b) is a potent scavenger of reactive oxygen species (ROS), which induces cell death during AR emergence (Steffens and Sauter, 2009). Gene expression assays revealed that the transcription of *BdUGT76-4* and *BdMT2b* genes was not

discernibly affected by wind treatments or falling down of the mesocotyls (Figures 31B and 31D). On the other hand, the transcription of *BdTAR2* gene was slightly induced by the same mechanical stimuli. However, auxin and NPA treatments did not discernibly affect the transcription of the genes (Figure 32). Overall, it is evident that auxin plays a primary role in the mechano-stimulation of AR formation by modulating the expression of *BdWOX* and *BdLBD* genes, which is in accordance with the effects of growth hormone inhibitors on AR formation (Figure 27). It seems that TAR2 is involved in the reprogramming process of root architecture in Brachypodium under wind conditions, as has been known in Arabidopsis (Ma et al., 2014).

Altogether, my findings illustrate a distinct auxin signaling pathway that mediates the wind-induced mechano-stimulation of AR formation in Brachypodium (Figure 31E). Under extreme wind conditions, plants fall down, resulting in the direct contact of the leaf nodes with soil particles. The mechanical stress imposed on the leaf nodes would trigger auxin accumulation/redistribution in the plant tissues. In this signaling scheme, the auxin signals induce the expression of *BdWOX* and *BdLBD* genes, finally leading to the induction of AR emergence. I propose that the auxin-mediated mechano-stimulation of AR development serves as an adaptive strategy, by which plants sustain their normal growth and productivity in extreme wind areas.

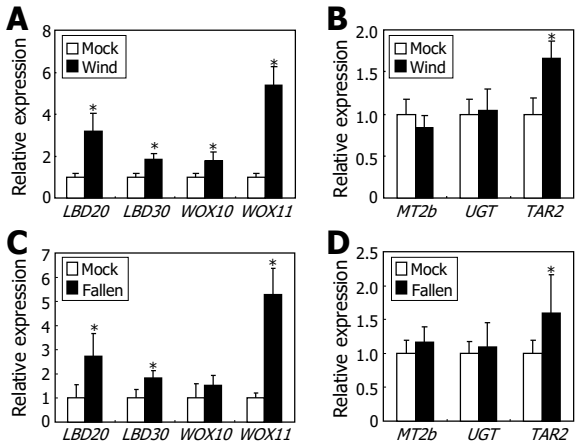

Figure 31. Induction of *WOX* and *LBD* genes by wind-mediated mechanical stimulation.

Following wind and mechanical stimulation, the leaf nodes and their internodes were harvested, and transcript levels were examined by RT-qPCR, as described in Figure 29B. The RT-qPCR data were normalized to an internal control, a gene encoding ubiquitin-conjugating enzyme 18. Biological triplicates, each consisting of 15 independent plants, were averaged (*t*-test, $*P < 0.01$). Error bars indicate SE.

(A and B) Transcription of *WOX* and *LBD* (**A**) and ethylene response (**B**) genes in wind-treated plants. Three-week-old plants grown in soil were exposed to wind flow for 6 hours.

(C and D) Transcription of *WOX* and *LBD* (**C**) and ethylene response (**D**) genes in fallen plants. Three-week-old plants grown in soil were artificially fallen down to the soil surface for 6 hours.

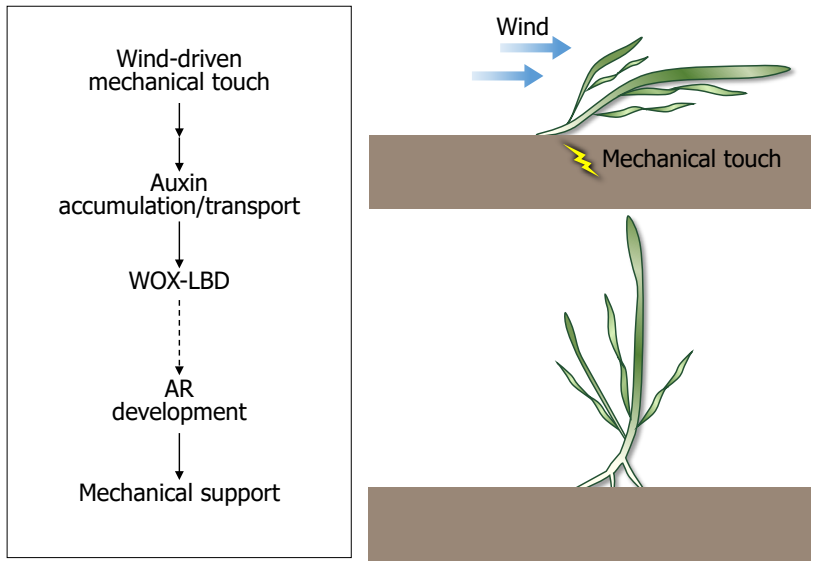

Figure 32. Schematic model of auxin-mediated AR formation under windy conditions.

In response to wind, plants fall down, imposing a mechanical stimuli on the leaf nodes. The mechanical stimulation triggers the accumulation and/or polar transport of auxin, which induces the expression of *WOX* and *LBD* genes. The WOX/LBD-mediated auxin signals triggers the initiation and development of ARs, leading to plant adaptation to mechanical stress.

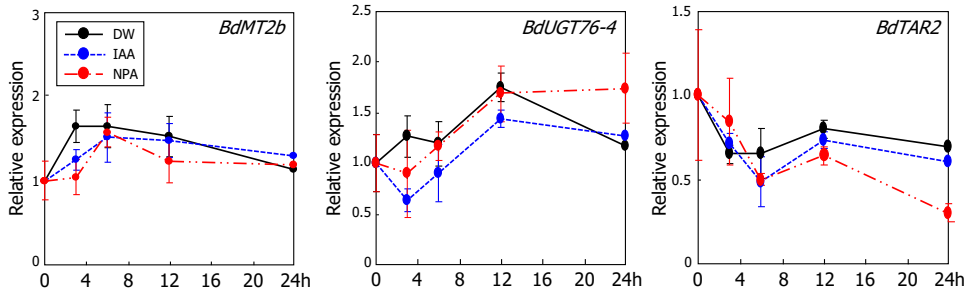

Figure 33. Effects of auxin and NPA on the transcription of ethylene-responsive genes.

Three-week-old plants grown in soil were artificially fallen down to the soil surface, and 0.1 mM IAA or 1 mM NPA solution was sprayed onto the aboveground plant parts. The leaf nodes and their internodes were harvested at the indicated time points for the extraction of total RNA. Transcript levels were analyzed by RT-qPCR. The data were normalized to an internal control, a gene encoding ubiquitin-conjugating enzyme 18. Biological triplicates, each consisting of 15 independent plants, were averaged. Error bars indicate SEM.

DISCUSSION

AR as an adaptive developmental device in response to environmental fluctuations

ARs are developmentally distinct from primary and lateral roots in that they are derived from nonroot tissues, such as root-shoot junction and stem nodes, through both normal developmental processes and stress response pathways prominently in grasses and cereal crops (Steffens and Rasmussen, 2016). Not only the economic and ecological values of ARs but also their importance as food sources are becoming apparent over the past decades. Economically, cut AR parts are capable of producing new individuals and thus frequently used in horticulture industries. Moreover, ARs play critical roles in plant adaptive processes under changing environments, underscoring their economic values in agricultural industry.

It is well-known that ARs help plants survive under certain abiotic and biotic stress conditions, such as flooding and nutrient deficiency frequently encountered in nature (Simberloff et al., 1978; Yu et al., 2014). The most extensively studied is submergence of plants in agricultural and natural ecosystems, often accompanying oxygen deficiency in plants. Rice is a semiaquatic plant that readily generates ARs upon flooding, and molecular signaling events leading to the stimulation of AR formation during flooding have been intensively studied

(Steffens et al., 2006; Vidoz et al., 2010; Nguyen et al., 2018). Submergence induces ethylene biosynthesis, and the gaseous growth hormone ethylene is trapped by water barrier. The accumulated ethylene triggers the production of ROS, which, in conjunction with ethylene, triggers epidermal programmed cell death for the induction of AR emergence (Steffens and Sauter, 2009).

The initiation and development of ARs vary widely depending on nutrient and stress types and root types. For example, the density of lateral roots originated in the pericyclic cells of crown roots increases when exposed to locally high concentrations of nitrate, while those originated from seminal roots are unaffected under similar nutrient conditions in maize (Yu et al., 2014; Yu et al., 2015). It is known that various root types that formed in different soil depths have differential efficiency of nutrient uptakes because nutrients are frequently distributed unevenly in relation to the soil layers. One typical example is uptake of phosphorus, which is available primarily in the soil surface layer. Therefore, while an increased number of surface roots enhances tolerance to phosphorus deficiency, deeper roots only poorly respond to phosphorus-deficient soil (Bonser et al., 1996). These phenomena highlight the complex regulation of AR emergence and growth under diverse nutrient-deficient conditions.

Hormonal regulation of post-embryonic root formation

AR organogenesis is modulated via a coordinated interaction of various hormonal networks. Generally, auxin plays a major role during the post-embryonic root formation (Casimiro et al., 2001). In Arabidopsis, it is well-established that auxin controls lateral root formation (Casimiro et al., 2001; De Smet et al., 2007; De Smet et al., 2010). Polar auxin transport is necessary for the organization of lateral root primordium. Auxin also play essential roles throughout the initiation and elongation of lateral roots by modulating auxin-responsive transcription factors and trafficking of PIN-FORMED (PIN) auxin transporters (Dubrovsky et al., 2008). In rice, it has been demonstrated that auxin flow through the PIN transporters is critical for the induction of AR emergence (Xu et al., 2005).

Other growth hormones, such as cytokinins, strigolactones, brassinosteroids, jasmonic acid (JA), abscisic acid (ABA), and gibberellic acid (GA), are also involved in the induction of AR formation (Jung and McCouch., 2013). For example, auxin signals activate genes encoding Gretchen Hagen 3-like proteins, which sustain JA homeostasis during AR formation (Gutierrez et al., 2012). It is known that cytokinin and auxin function antagonistically in regulating AR formation (Ramírez-Carvajal et al., 2009). Meanwhile, ABA inhibits GA and ethylene signaling in the course of AR emergence and elongation (Steffens et al., 2006).

In this study, I demonstrated that Brachypodium efficiently adapts to wind

stress, in which wind-induced mechanical stimulation promotes AR formation via a WOX/LBD-mediated auxin signaling pathway. Phylogenetic analysis, gene expression studies, and transcriptional responses to mechanical stimuli identified a subset of Brachypodium *WOX*/*LBD* genes that are involved in the auxin-mediated mechanical stress adaptation. These genes are expressed in the leaf nodes, from which ARs are formed, and the gene transcription is further induced upon exposure to wind and mechanical falling down of the mesocotlys. It was found that the induction of *WOX*/*LBD* genes did not occur in NPA-treated plants, indicating that auxin transport is important for the WOX/LBD-mediated mechanical adaptation process. It is currently unclear how the wind-mediated mechanical stimuli are linked with auxin signaling at the molecular level. It is possible that both auxin transport and its biosynthesis, and perhaps auxin sensitivity as well, would be involved in the wind-induced mechanical stress responses. Functional identification of auxin biosynthetic enzymes and wind/mechanical stimuli-responsive PIN proteins and direct measurements of endogenous contents under mechanical stress conditions would help elucidate the underlying molecular mechanisms.

The *TAR2* gene, an ethylene response marker gene (Kouzai et al., 2016), was induced slightly by wind exposure. Meanwhile, NPA treatments decreased its transcription, while auxin does not have any effects on the gene transcription. The

Arabidopsis *TAR2* gene encodes a tryptophan aminotransferase that mediates auxin biosynthesis in response to ET signaling (Stepanova et al., 2008). It has been reported that the Arabidopsis *TAR2* gene is required for the emergence of lateral roots under low nitrogen stress conditions (Ma et al., 2014). It is envisioned that TAR2-mediated ET signals do not play a direct role in the wind-induced thigmomorphogenic adaptation process but instead affect indirectly the AR formation by affecting auxin biosynthesis.

In accordance with the seemingly limited role of the ET response markers, UGT76-4 and TAR2, assays with ET perception inhibitor showed that wind-induced AR formation is not discernibly affected by ET signaling. Treatments with the ET perception inhibitor $AgNO_3$ slightly induces AR emergence. However, the chemical treatments do not exhibit any dosage effects on the incidence of AR emergence. It is thus assumed that the marginal effects of $AgNO_3$ on AR formation might be caused by a side effect of the chemical during plant morphogenesis (Kumar et al., 2009). Nevertheless, it is still possible that ET might play a certain role in the thigmomorphogenic AR formation through as-yet unidentified signaling crosstalks with auxin. Further works using Brachypodium mutants having defects in auxin and ET biosynthesis or signaling and genome-wide gene expression studies would be of great helps to explore the possibility.

Induction of AR development by mechanical stimuli

Mechano-stimulation of AR formation has been reported in rice (Steffens et al., 2012). The gaseous growth hormone ET promotes ROS accumulation by suppressing the function of the ROS scavenger MT2b. External or internal mechanical pressure simultaneously promotes epidermal cell death, which facilitates the emergence of ARs. The two mutually collaborative signals provide an elaborative spatiotemporal information to initiate ARs in appropriate nonroot tissues in rice.

My findings showed that wind-mediated mechanical stimulation does not alter the expression of the Brachypodium *MT2b* gene, indicating that the wind-mediated thermomorphogenic AR development in Brachypodium differs from the ROS-mediated mechanical stimulation of AR emergence in rice. A critical issue is as to cellular receptors or sensory molecules that are capable of perceiving mechanical signals. One such potential candidate is cytosolic Ca^{2+} ion, a ubiquitously conserved signaling component in all living organisms (Trewavas and Knight, 1994; Marchadier et al., 2016).

It has been observed that mechanical perturbations are immediately followed by rapid increase in cytosolic Ca^{2+} concentrations in a dose-dependent manner in *Nicotiana plumbaginifolia* (Knight et al., 1992). The Arabidopsis and rice genomes possess ten and five mechano-sensitive Ca^{2+} ion channels,

respectively, supporting the involvement of Ca^{2+} ion as a sensing molecule or second messenger in the mechano-adaptation process (Haswell et al., 2008). Intriguingly, it is known that the Ca^{2+}-permeable mechano-sensitive channel 1 (MCA1) mediates Ca^{2+} uptake in response to agar hardness on culture media in Arabidopsis (Nakagawa et al., 2007). Overall, it is now apparent that thigmomorphogenic response is a critical adaptation process to cope with mechano-disturbing environmental stresses, while underlying signaling schemes and molecular mechanisms are to be investigated in the future.

There is a steadily increasing concern about wind-induced damages on plant ecosystems and crop productivity, and thus further understanding molecular mechanisms underlying the wind-induced thigmomorphogenic adaptation in agricultural crops is an important issue in the field. Under these circumstances, my findings would contribute to further elucidating the molecular signaling cascades of AR development that are readily applicable to developing mechano-resistant crops in the future.

ACKNOWLEDGEMENTS

I thank Hyo-Jun Lee for technical assistance. Bo Eun Nam performed the gene expression analysis experiments.

REFERENCES

Arsovski, A.A., Galstyan, A., Guseman, J.M., and Nemhauser, J.L. (2012). Photomorphogenesis. Arabidopsis Book doi: 10.1199/tab.0147.

Badel, E., Ewers, F.W., Cochard, H., and Telewski, F.W. (2015). Acclimation of mechanical and hydraulic functions in trees: impact of the thigmomorphogenetic process. Frontiers in Plant Science **6:** 1-12.

Baudry, A., et al. (2010). F-Box proteins FKF1 and LKP2 act in concert with ZEITLUPE to control *Arabidopsis* clock progression. Plant Cell **22:** 606-622.

Beyer, E.M. (1976). A potent inhibitor of ethylene action in plants. Plant Physiology **58:** 268-271.

Bita, C.E., and Gerats, T. (2013). Plant tolerance to high temperature in a changing environment: scientific fundamentals and production of heat stress-tolerant crops. Front. Plant Sci. **4:** 273.

Biddington, N.L. (1986). The effects of mechanically-induced stress in plants: a review. Plant Growth Regulation **4:** 103-123.

Bonser, A.M, Lynch, J., and Snapp, S. (1996). Effect of phosphorus deficiency on growth angle of basal roots in *Phaseolus vulgaris*. New Phytologist **132:** 281-288.

Borkovich, K.A., Farrelly, F.W., Finkelstein, D.B., Taulien, J., and Lindquist, S. (1989). Hsp82 is an essential protein that is required in higher concentrations for growth of cells at higher temperatures. Mol. Cell. Biol. **9:** 3919-3930.

Braam, J., and Davis, R.W. (1990). Rain-, wind-, and touch-induced expression of calmodulin and calmodulin-related genes in *Arabidopsis*. Cell **60:** 357-364.

Brkljacic, J., et al. (2011). *Brachypodium* as a model for the grasses: today and the future. Plant Physiology **157:** 3-13.

Casimiro, I., et al. (2001). Auxin transport promotes Arabidopsis lateral root initiation. The Plant Cell **13:** 843-852.

Cha, J.Y., Kim, M.R., Kim, W.Y., and Kim, M.G. (2015). Development of *in vitro* HSP90 foldase chaperone assay using a GST-fused real-substrate, ZTL (ZEITLUPE). J. Plant Biol. **58:** 236-241.

Chehab, E.W., Eich, E., and Braam, J. (2009). Thigmomorphogenesis: a complex plant response to mechano-stimulation. Journal of Experimental Botany **60:** 43-56.

Coll, N.S., Smidler, A., Puigvert, M., Popa, C., Valls, M., and Dangl, J.L. (2014). The plant metacaspase AtMC1 in pathogen-triggered programmed cell death and aging: functional linkage with autophagy. Cell Death Differ. **21:** 1399-1408.

Coutand, C., Dupraz, C., Jounen, G., Ploquin, S., and Adam, B. (2008).

Mechanical stimuli regulate the allocation of biomass in trees: demonstration with young *Prunus avium* trees. Annals of Botany **101:** 1421-1432.

De Smet, I., et al. (2007). Auxin-dependent regulation of lateral root positioning in the basal meristem of Arabidopsis. Development **134:** 681-690.

Dickey, C.A., et al. (2007). The high-affinity HSP90-CHIP complex recognizes and selectively degrades phosphorylated tau client proteins. J. Clin. Invest. **117:** 648-658.

Dubrosky, J.G., Sauer, M., Napsucialy-Mendivil, S., Ivanchenko, M.G., Friml, J., Shishkova, S., Celenza, J., and Benková, E. (2008). Auxin acts as a local morphogenetic trigger to specify lateral root founder cells. Proceedings of the National Academy of Sciences of United States of America **105:** 8790-8794.

Edwards, K.D., Lynn, J.R., Gyula, P., Nagy, F., and Millar, A.J. (2005). Natural allelic variation in the temperature-compensation mechanisms of the *Arabidopsis* thaliana circadian clock. Genetics **170:** 387-400.

Fang, N.N., Ng, A.H., Measday, V., and Mayor, T. (2011). Hul5 HECT ubiquitin ligase plays a major role in the ubiquitylation and turnover of cytosolic misfolded proteins. Nat. Cell Biol. **13:** 1344-1352.

Farré, E.M., Harmer, S.L., Harmon, F.G., Yanovsky, M.J., and Kay, S.A. (2005). Overlapping and distinct roles of PRR7 and PRR9 in the *Arabidopsis* circadian clock. Curr. Biol. **15:** 47-54.

Filichkin, S.A., Cumbie, J.S., Dharmawardhana, P., Jaiswal, P., Chang, J.H., Palusa, S.G., Reddy, A.S., Megraw, M., and Mockler, T.C. (2015). Environmental stresses modulate abundance and timing of alternatively spliced circadian transcripts in *Arabidopsis*. Mol. Plant **8:** 207-227.

Finka, A., and Goloubinoff, P. (2013). Proteomic data from human cell cultures refine mechanisms of chaperone-mediated protein homeostasis. Cell Stress Chaperones **18:** 591-605.

Finka, A., Sood, V., Quadroni, M., Rios, P.L., and Goloubinoff, P. (2015). Quantitative proteomics of heat-treated human cells show an across-the-board mild depletion of housekeeping proteins to massively accumulate few HSPs. Cell Stress Chaperones **20:** 605-620.

Gardiner, B., Berry, P., and Moulia, B. (2016). Review: wind impacts on plant growth, mechanics and damage. Plant Science **245:** 94-118.

Gillies, J.A., Nickling, W.G., and King, J. (2002). Drag coefficient and plant form response to wind speed in three plant species: burning bush (*Euonymus alatus*), Colorado blue spruce (*Picea pungens* glauca.), and fountain grass (*Pennisetum setaceum*). Climate and Dynamics **107:** ACL 10-1-ACL10-15.

Gutierrez, L., et al. (2008). The lack of a systematic validation of reference genes: a serious pitfall undervalued in reverse transcription-polymerase chain reaction (RT-PCR) analysis in plants. Plant Biotechnol. J. **6:** 609-618.

Gutierrez, L., et al. (2012). Auxin controls Arabidopsis adventitious root initiation by regulating jasmonic acid homeostasis. Plant Cell **24:** 2515-2527.

Haswell, E.S., Peyronnet, R., Barbier-Brygoo, H., Meyerowitz, E.M., and Frachisse, J-M. (2008). Two MscS homologs provide mechanosensitive channel activities in the Arabidopsis root. Cell **18:** P730-P734.

Heck, J.W., Cheung, S.K., and Hampton, R.Y. (2010). Cytoplasmic protein quality control degradation mediated by parallel actions of the E3 ubiquitin ligases Ubr1 and San1. Proc. Natl Acad. Sci. USA **107:** 1106-1111.

Huett, A., Heath, R.J., Begun, J., Sassi, S.O., Baxt, L.A., Vyas, J.M., Goldberg, M.B., and Xavier, R.J. (2012). The LRR and RING domain protein LRSAM1 is an E3 ligase crucial for ubiquitin-dependent autophagy of intracellular Salmonella Typhimurium. Cell Host Microbe **12:** 778-790.

Imai, J., Maruya, M., Yashiroda, H., Yahara, I., and Tanaka, K. (2003). The molecular chaperone Hsp90 plays a role in the assembly and maintenance of the 26S proteasome. EMBO J. **22:** 3557-3367.

Jaffe, M.J., and Forbes, S. (1993). Thigmomorphogenesis: the effect of mechanical perturbation on plants. Plant Growth Regulation **12:** 313-324.

Jung, J.K., and McCouch, S. (2013). Getting to the roots of it: genetic and hormonal control of root architecture. Frontiers in Plant Sciences **4:** 186.

Kellermann, O., and Szmelcman, S. (1974). Active transport of maltose in *Escherichia coli* K12. Involvement of a "periplasmic" maltose binding protein. Eur. J. Biochem. **47:** 139-149.

Kiba, T., Henriques, R., Sakakibara, H., and Chua, N.H. (2007). Targeted degradation of PSEUDO-RESPONSE REGULATOR5 by an SCF^{ZTL} complex regulates clock function and photomorphogenesis in *Arabidopsis thaliana*. Plant Cell **19:** 2516-2530.

Kim, T.S., Kim, W.Y., Fujiwara, S., Kim, J., Cha, J.Y., Park, J.H., Lee, S.Y., and Somers, D.E. (2011). HSP90 functions in the circadian clock through stabilization of the client F-box protein ZEITLUPE. Proc. Natl Acad. Sci. USA **108:** 16843-16848.

Kim, W.Y., Geng, R., and Somers, D.E. (2003). Circadian phase-specific degradation of the F-box protein ZTL is mediated by the proteasome. Proc. Natl Acad. Sci. USA **100:** 4933-4938.

Knight, M.R., Smith, S.M., and Trewavas, A.J. (1992). Wind-induced plant motion immediately increases cytosolic calcium. Proceedings of the National Academy of Sciences of United States of America **89:** 4967-4971.

Kouzai, Y., et al. (2016). Expression profiling of marker genes responsive to the defence-associated phytohormones salicylic acid, jasmonic acid and ethylene in *Brachypodium distachyon*. BMC plant biology. **16:** 59.

Krishna, P., and Gloor, G. (2001). The Hsp90 family of proteins in *Arabidopsis thaliana*. Cell Stress Chaperones **6:** 238-246.

Kumar, V., Parvatam, G., and Ravishankar, G.A. (2009). $AgNO_3$-a potential regulator of ethylene activity and plant growth modulator. Electronic Journal of Biotechnology doi: 10.2225/vol12-issue2-fulltext-1.

Lata, C., and Prasad, M. (2011). Role of DREBs in regulation of abiotic stress responses in plants. J. Exp. Bot. **62:** 4731-4748.

Lee, D.H., and Goldberg, A.L. (1998). Proteasome inhibitors: valuable new tools for cell biologists. Trends Cell Biol. **8:** 397-403.

Lee, S., Lee, D.W., Lee, Y., Mayer, U., Stierhof, Y.D., Lee, S., Jürgens, G., and Hwang, I. (2009). Heat shock protein cognate 70-4 and an E3 ubiquitin ligase, CHIP, mediate plastid-destined precursor degradation through the ubiquitin-26S proteasome system in *Arabidopsis*. Plant Cell **21:** 3984-4001.

Lee, S., Seo, P.J., Lee, H.J., and Park, C.M. (2012). A NAC transcription factor NTL4 promotes reactive oxygen species production during drought-induced leaf senescence in *Arabidopsis*. Plant J. **70:** 831-844.

Liu, H., Wang, S., Yu, X., Yu, J., He, X., Zhang, S., Shou, H., and Wu, P. (2005). ARL1, a LOB-domain protein required for adventitious root formation in rice. The Plant Journal **43:** 47-56.

Liu, J., Sheng, L., Xu, Y., Li, J., Yang, Z., Huang, H., and Xu, L. (2014).

WOX11 and *12* are involved in the first-step cell fate transition during de novo root organogenesis in Arabidopsis. Plant Cell **26:** 1081-1093.

Ma, W., Li, J., Qu, B., He, X., Zhao, X., Li, B., Fu, X., and Tong, Y. (2014). Auxin biosynthetic gene *TAR2* is involved in low nitrogen-mediated reprogramming of root architecture in Arabidopsis. The Plant Journal **78:** 70-79.

Marchadier, E., Oates, M.E., Fang, H., Donoghue, P.C.J., Hetherington, A.M., and Gough, J. (2016). Evolution of the calcium-based intracellular signaling system. Genome Biology and Evolution **8:** 2118-2132.

Marcolino-Gomes, J., et al. (2014). Diurnal oscillations of soybean circadian clock and drought responsive genes. PLoS ONE **9:** e86402.

Martin-Tryon, E.L., Kreps, J.A., and Harmer, S.L. (2007). GIGANTEA acts in blue light signaling and has biochemically separable roles in circadian clock and flowering time regulation. Plant Physiol. **143:** 473-486.

Más, P., Kim, W.Y., Somers, D.E., and Kay, S.A. (2003). Targeted degradation of TOC1 by ZTL modulates circadian function in *Arabidopsis thaliana*. Nature **426:** 567-570.

McClellan, A. J., Tam, S., Kaganovich, D., and Frydman, J. (2005). Protein quality control: chaperones culling corrupt conformations. Nat. Cell Biol. **7:** 736-741.

Meiri, D., and Breiman, A. (2009). *Arabidopsis* ROF1 (FKBP62) modulates thermotolerance by interacting with HSP90.1 and affecting the accumulation of HsfA2-regulated sHSPs. Plant J. **59:** 387-399.

Mi C, Zhang X, Li S, Yang J, Zhu D, Yang Y. (2011). Assessment of environment lodging stress for maize using fuzzy synthetic evaluation. Mathematical and Computer Modeling **54:** 1053-1060.

Mimnaugh, E.G., Xu, W., Vos, M., Yuan, X., Isaacs, J.S., Bisht, K.S., Gius, D., and Neckers, L. (2004). Simultaneous inhibition of hsp 90 and the proteasome promotes protein ubiquitination, causes endoplasmic reticulum-derived cytosolic vacuolization, and enhances antitumor activity. Mol. Cancer Ther. **3:** 551-566.

Mitchell, S.J. (2013). Wind as a natural disturbance agent in forests: a synthesis. Forestry **86:** 147-157.

Nakagawa, Y., et al. (2007). Arabidopsis plasma membrane protein crucial for Ca^{2+} influx and touch sensing in roots. Proceedings of the National Academy of Sciences of United States of America **104:** 3639-3644.

Nguyen, T-N., Tuan, P.A., Mukherjee, S., Son, S., and Avele, B.T. (2018). Hormonal regulation in adventitious roots and during their emergence under waterlogged conditions in wheat. Journal of Experimental Botany **69:** 4065-4082.

Norén, L., Kindgren, P., Stachula, P., Rühl, M., Eriksson, M.E., Hurry, V., and Strand, Å. (2016). Circadian and plastid signaling pathways are integrated to ensure correct expression of the CBF and COR genes during photoperiodic growth. Plant Physiol. **171:** 1392-1406.

Ottenschläger, I., Wolff, P., Wolverton, C., Bhalerao, R.P., Sandberg, G., Ishikawa, H., Evans, M., and Palme, K. (2003). Gravity-regulated differential auxin transport from columella to lateral root cap cells. Proceedings of the National Academy of Sciences of United States of America **100:** 2987-2991.

Panchuk, I.I., Volkov, R.A., and Schöffl, F. (2002). Heat stress- and heat shock transcription factor-dependent expression and activity of ascorbate peroxidase in *Arabidopsis*. Plant Physiol. **129:** 838-853.

Poiré, R., Chochois, V., Sirault, X.R., Vogel, J.P., Watt, M., and Furbank, R.T. (2014). Digital imaging approaches for phenotyping whole plant nitrogen and phosphorus response in *Brachypodium distachyon*. Journal of Integrative Plant Biology **56:** 781-796.

Pratt, W.B., Morishima, T., Peng, H.M., and Osawa, Y. (2010). Proposal for a role of the Hsp90/Hsp70-based chaperone machinery in making triage

decisions when proteins undergo oxidative and toxic damage. Exp. Biol. Med. **235:** 278-289.

Quint, M., Delker, C., Franklin, K.A., Wigge, P.A., Halliday, K.J., and van Zanten, M. (2016). Molecular and genetic control of plant thermomorphogenesis. Nature Plants **2:** 15190.

Ramírez-Carvajal, G.A., Morse, A.M., Dervinis, C., and Davis, J.M. (2009). The cytokinin type-B response regulator *PtRR13* is a negative regulator of adventitious root development in Populus. Plant Physiology **150:** 759-771.

Reubens, B., Pannemans, B., Danjon, F., De Profit, M., De Baets, S., De Baerdemaeker, J., Poesen, J., and Muys, B. (2009). The effect of mechanical stimulation on root and shoot development of young containerised *Quercus robur* and *Robinia pseudoacacia* trees. Trees **23:** 1213.

Sabatini, S., et al. (1999). An auxin-dependent distal organizer of pattern and polarity in the Arabidopsis root. Cell **99:** 463-472.

Samant, R.S., Clarke, P.A., and Workman, P. (2014). E3 ubiquitin ligase Cullin-5 modulates multiple molecular and cellular responses to heat shock protein 90 inhibition in human cancer cells. Proc. Natl Acad. Sci. USA **111:** 6834-6839.

Sangster, T.A., Salathia, N., Lee, H.N., Watanabe, E., Schellenberg, K., Morneau, K., Wang, H., Undurraga, S., Queitsch, C., and Lindquist, S.

(2008). HSP90-buffered genetic variation is common in *Arabidopsis thaliana*. Proc. Natl Acad. Sci. USA **105:** 2969-2974.

Sangster, T.A., and Queitsch, C. (2005). The HSP90 chaperone complex, an emerging force in plant development and phenotypic plasticity. Curr. Opin. Plant Biol. **8:** 86-92.

Sarquis, J.I., Jordan, W.R., and Morgan, P.W. (1991). Ethylene evolution from maize (*Zea mays* L.) seedling roots and shoots in response to mechanical impedance. Plant Physiology **96:** 1171-1177.

Schneider, R., Linka, R.M., and Reinke, H. (2014). HSP90 affects the stability of BMAL1 and circadian gene expression. J. Biol. Rhythms **29:** 87-96.

Seo, P.J., Park, M.J., Lim, M.H., Kim, S.G., Lee, M., Baldwin, I.T., and Park, C.M. (2012). A self-regulatory circuit of CIRCADIAN CLOCK-ASSOCIATED1 underlies the circadian clock regulation of temperature responses in *Arabidopsis*. Plant cell **24:** 2427-2442.

Shah, A.N., Tanveer, M., Rehman, A.U., Anjum, S.A., Iqbal, J., and Ahmad, R. (2017). Lodging stress in cereal-effects and management: an overview. Environmental Science and Pollution Research **24:** 5222-5237.

Shirasu, K. (2009). The HSP90-SGT1 chaperone complex for NLR immune sensors. Annu. Rev. Plant Biol. **60:** 139-164.

Simberloff, D., Brown, B.J., and Lowrie, S. (1978). Isopod and insect root borers

may benefit Florida mangroves. Science **201:** 630-632.

Steffens, B., Kovalev, A., Gorb, S.N., and Sauter, M. (2012). Emerging roots alter epidermal cell fate through mechanical and reactive oxygen species signaling. Plant Cell **24:** 3296-3306.

Steffens, B., and Rasmussen, A. (2016). The physiology of adventitious roots. Plant Physiology **170:** 603-617.

Steffens, B., and Sauter, M. (2009). Epidermal cell death in rice is confined to cells with a distinct molecular identity and is mediated by ethylene and H_2O_2 through an autoamplified signal pathway. Plant Cell **21:** 184-196.

Steffens, B., Wang, J., and Sauter, M. (2006). Interactions between ethylene, gibberellin and abscisic acid regulate emergence and growth rate of adventitious roots in deepwater rice. Planta **223:** 604-612.

Stepanova, A.N., Robertson-Hoyt, J., Yun, J., Benavente, L.M., Xie, D.Y., Dolezal, K., Schlereth, A., Jürgens, G., and Alonso, J.M. (2008). TAA1-mediated auxin biosynthesis is essential for hormone crosstalk and plant development. Cell **133:** 177-191.

Takahashi, H., and Jaffe, M.J. (1984). Thigmomorphogenesis: the relationship of mechanical perturbation to elicitor-like activity and ethylene production. Physiologia Plantarum **61:** 405-411.

Taldone, T., Sun, W., and Chiosis, G. (2009). Discovery and development of heat shock protein 90 inhibitors. Bioorg. Med. Chem. **17:** 2225-2235.

Tamaru, T., et al. (2013). ROS stress resets circadian clocks to coordinate pro-survival signals. PLoS ONE **8:** e82006.

Thomson, K.S., Hertel, R., Müller, S., and Tavares, J.E. (1973). 1-N-naphthylphthalamic acid and 2, 3, 5-triiodobenzoic acid. Planta **109:** 337-352.

Trewavas, A., and Knight, M. (1994). Mechanical signaling, calcium and plant form. Plant Molecular Biology **5:** 1329-1341.

Urban, S.T., Lieffers, V.J., and Macdonald, S.E. (1994). Release in radial growth in the trunk and structural roots of white spruce as measured by dendrochronology. Canadian Journal of Forest Research **24:** 1550-1556.

Vidoz, M.L., Loreti, E., Mensuali, A., Alpi, A., and Perata, P. (2010). Hormonal interplay during adventitious root formation in flooded tomato plants. The Plant Journal **63:** 551-562.

von Koskull-Döring, P., Scharf, K.D., and Nover, L. (2007). The diversity of plant heat stress transcription factors. Trends Plant Sci. **12:** 452-457.

Wang, X., Li, X., and Li, Y. (2007). A modified Coomassie Brilliant Blue staining method at nanogram sensitivity compatible with proteomic analysis. Biotechnol. Lett. **29:** 1599-1603.

Xu, M., Zhu, L., Shou, H., and Wu, P. (2005). A *PIN1* family gene, *OsPIN1*,

involved in auxin-dependent adventitious root emergence and tillering in rice. Plant & Cell Physiology **46:** 1674-1681.

Xu, Z.S., Li, Z.Y., Chen, Y., Chen, M., Li, L.C., and Ma, Y.Z. (2012). Heat shock protein 90 in plants: molecular mechanisms and roles in stress responses. Int. J. Mol. Sci. **13:** 15706-15723.

Yamamoto, Y., Sato, E., Shimizu, T., Nakamich, N., Sato, S., Kato, T., Tabata, T., Nagatani, A., Yamashino, T., and Mizuno, T. (2003). Comparative genetic studies on the APRR5 and APRR7 genes belonging to the APRR1/TOC1 quintet implicated in circadian rhythm, control of flowering time, and early photomorphogenesis. Plant Cell Physiol. **44:**1119-1130.

Yoo, C.Y., Miura, K., Jin, J.B., Lee, J., Park, H.C., Salt, D.E., Yun, D.J., Bressan, R.A., and Hasegawa, P.M. (2006). SIZ1 small ubiquitin-like modifier E3 ligase facilitates basal thermotolerance in *Arabidopsis* independent of salicylic acid. Plant Physiol. **142:** 1548-1558.

Yoo, Y. S., et al. (2015). The mitochondrial ubiquitin ligase MARCH5 resolves MAVS aggregates during antiviral signaling. Nat. Commun. **6:**7910 doi:10.1038/ncomms8910.

Yu, P., Eggert, K., von Wirén, N., Li, C., and Hochholdinger, F. (2015). Cell-type specific gene expression analyses by RNA-Seq reveal local high nitrate triggered lateral root initiation in shoot-borne roots of maize by modulating

auxin-related cell cycle-regulation. Plant Physiology **169:** 690-704.

Yu, P., White, P.J., Hochholdinger, F., and Li, C. (2014). Phenotypic plasticity of the maize root system in response to heterogeneous nitrogen availability. Planta **240:** 667-678.

Zhao, Y., Hu, Y., Dai, M., Huang, L., and Zhou, D.X. (2009). The *WUSCHEL*-related homeobox gene *WOX11* is required to activate shoot-borne crown root development in rice. The Plant Cell **21:** 736-748.

Zhou, J., Wang, J., Cheng, Y., Chi, Y.J., Fan, B., Yu, J.Q., and Chen, Z. (2013). NBR1-mediated selective autophagy targets insoluble ubiquitinated protein aggregates in plant stress responses. PLoS Genet. **9:** e1003196.

Zhou, J., Zhang, Y., Qi, J., Chi, Y., Fan, B., Yu, J.Q., and Chen, Z. (2014). E3 ubiquitin ligase CHIP and NBR1-mediated selective autophagy protect additively against proteotoxicity in plant stress responses. PLoS Genet. **10:** e1004116.

Zielinski, T., Moore, A.M., Troup, E., Halliday, K.J., and Millar, A.J. (2014). Strengths and limitations of period estimation methods for circadian data. PLoS ONE **9:** e96462.

Zuehlke, A., and Johnson, J.L. (2010). Hsp90 and co-chaperones twist the functions of diverse client proteins. Biopolymers **93:** 211-217.

PUBLICATION LIST

1. **Park, M.J., Kwon, Y.J., Gil, K.E., and Park, C.M.** (2016). LATE ELONGATED HYPOCOTYL regulates photoperiodic flowering via the circadian clock in *Arabidopsis*. *BMC Plant Biol.* **16:** 114-125.

2**. Gil, K.E., Park, M.J., Lee, H.J., Park, Y.J., Han, S.H., Kwon, Y.J., Seo, P.J., Jung, J.H., and Park, C.M.** (2017). Alternative splicing provides a proactive mechanism for the diurnal CONSTANS dynamics in *Arabidopsis* photoperiodic flowering. *Plant J.* **89:** 128-140.

3. **Gil, K.E., Kim, W.Y., Lee, H.J., Faisal, M., Saquib, Q., Alatar, A.A., and Park, C.M.** (2017). ZEITLUPE contributes to a thermoresponsive protein quality control system in *Arabidopsis*. *Plant cell* **29:** 2882-2894.

4. **Gil, K.E., Ha, J.H., and Park, C.M.** (2018). Abscisic acid-mediated phytochrome B signaling promotes primary root growth in *Arabidopsis*. *Plant Signaling & Behavior* **13:** 5-8.

5. **Gil, K.E., and Park, C.M**. (2019). Thermal adaptation and plasticity of the plant circadian clock. *New Phytol*. **221:** 1215-1229.

6. **Park, Y.J., Lee, H.J., Gil, K.E.,** et al., (2019). Developmental programming of thermonastic leaf movement. *Plant physiol.* DOI: 10.1104/pp.19.00139.

ABSTRACT IN KOREAN

식물은 주변 환경의 영향을 받는다는 것이 잘 알려져 있다. 대표적인 환경적 자극 요인으로는 빛과 온도의 변동, 바람이나 홍수, 동물의 움직임에 의한 물리적인 자극 등이 있다. 식물은 환경적 자극에 대응하여 다양한 적응 전략을 발달시켜왔다. 예를 들어, 생체시계는 외부의 환경 변화를 예측하고 인지함으로써 식물 내의 다양한 생리 발달 과정을 조절하고 식물의 생장을 최적화한다. 본 연구에서는 이러한 생체시계의 열 안정성과 관련된 분자 기작에 대해서 알아보았다.

한편, 접촉이나 바람과 같은 환경적 자극은 생체 시계뿐만 아니라 외형의 변화를 유도하기도 한다. 이러한 물리적 자극에 의한 외형적 변화를 접촉형태형성(thigmomorphogenesis)이라고 한다. 본 연구에서는 바람에 의한 숲개밀의 뿌리 형성에 대한 표현형을 분석하고, 외떡잎식물의 뿌리 발달 기작을 기반으로 호르몬의 조절 방법에 대해서 논의하였다.

제 1 장에서는 열 스트레스 하에서 ZEITLUPE (ZTL)의 protein quality control 기능에 대해 다루었다. 세포 단백질은 고온 스트레스 하에서 변성 및 산화에 의한 손상을 받아 세포 내에 독성을 가지는 불용성 응집체를 형성한다. 변성된 단백질은 원래의 형태로 재생되거나 세포질 구획에서 제거된다. 이 과정을 protein quality control 이라고 하며,

heat shock protein (HSP)은 변성된 단백질 재생 과정을 돕는 분자 샤페론 역할을 한다. 본 연구에서는 고온에 의해 변성된 단백질 응집체가 애기장대의 생체시계 조절 인자인 ZTL 에 의한 protein quality control 기작에 의해 제거됨을 증명하였다. ZTL 은 변성된 단백질을 polyubiquitination 시킴으로써 proteasomal degradation 과정으로 유도한다. ZTL 이 없는 돌연변이체(*ztl*)에서는 고온에 의해 유도되는 polyubiquitination 이 충분히 일어나지 못하므로 insoluble 한 단백질 응집체가 더욱 많이 쌓이게 되며, 고온에 취약한 표현형을 보인다. 또한, *ztl* 돌연변이체가 고온에서 생체시계 리듬이 깨지는 현상을 관찰한 바, ZTL 을 통한 protein quality control 이 식물 생체시계의 고온 안정성에 기여한다고 제안하였다. 나아가 샤페론인 HSP90 과 ZTL 단백질의 interaction 이 고온에서도 유지되며, HSP90 의 발현이 낮은 식물체의 polyubiquitination 정도와 생체시계 리듬의 고온 반응성이 *ztl* 돌연변이체와 유사한 양상을 보인다는 것을 통해 HSP90 과 ZTL 이 기능적인 측면에서 관련되어 있다는 것을 알 수 있었다.

제2 장에서는 부정근 형성에 대한 바람의 영향에 대해서 논의하였다. 바람에 의한 물리적 자극은 식물의 키를 작게 하고 방사형으로 넓고 튼튼하게 자라도록 한다. 또한 뿌리의 발달에서도 다양한 효과를 일으킨다고 알려져 있다. 그러나 식물이 어떤 기작으로 바람을 인지하고 적응 발달을 일으키는지는 알려지지 않았다. 본

연구에서는 외떡잎식물 종의 모델 식물인 숲개밀이 바람에 의한 자극에 적응하기 위해서 부정근을 형성한다는 것을 발견하였다. 부정근은 바람에 의한 식물체의 흔들림을 막고, 지면과 식물의 고착면을 넓힘으로써 뿌리가 안정적으로 식물을 지탱하도록 한다. 복합적인 환경적 자극인 바람을 물리적인 접촉 자극, 공기 압력 자극, 중력 자극 등으로 나누어 분석한 결과, 중경(mesocotyl)의 접힘 현상보다는 leaf node와 흙의 물리적 접촉이 부정근 형성을 유도한다는 것을 밝혔다. 또한, 오옥신과 에틸렌 신호 억제제를 처리한 후 식물의 부정근 형성 양상을 관찰함으로써, 에틸렌보다는 오옥신이 부정근의 접촉형태형성에 깊게 관여되어 있음을 알 수 있었다. 오옥신은 관련 유전자인 *WUSCHEL RELATED HOMEOBOX*와 *LATERAL ORGAN BOUNDARIES DOMAIN* 전사 인자들의 발현을 유도함으로써 바람에 의한 부정근 형성에 참여한다는 것을 밝혔다.

주요어: 부정근, 고온 스트레스, 단백질 품질 관리, 고온 저항성, 접촉형태형성, 바람

학 번: 2014-22389